Technischen Universität München
Institut für Pharmakologie und Toxikologie

Functional Analysis of Truncated Murine Cav1.2 at Asp-1904 in hearts

Jie Ding

Vollständiger Abdruck der von der Fakultät Wissenschaftszentrum Weihenstephan für Ernährung, Landnutzung und Umwelt der Technischen Universität München zur Erlangung des akademischen Grades eines

Doktors der Naturwissenschaften

genehmigten Dissertation.

Vorsitzende: Univ.-Prof. Dr.H. Daniel

Prüfer der Dissertation:

1. Univ.-Prof. Dr. M. Schemann
2. Univ.-Prof. Dr. F. Hofmann

Die Dissertation wurde am 19.12.2012 bei der Technischen Universität München eingereicht und durch die Fakultät Wissenschaftszentrum Weihenstephan für Ernährung, Landnutzung und Umwelt am 13.03.2013 angenommen.

Abbreviations

AC	adenylyl cyclase
AKAPs	A kinase anchoring proteins
aspartate	Asp
ATP	adenosine-5'-triphosphate
bp	base pair
BSA	bovine serum albumin
BTZs	benzothiazepines
cAMP	cyclic AMP
Ca^{2+}	calcium
CDF	Ca^{2+}-dependent facilitation
CDI	Ca^{2+}-dependent inactivation
cDNA	complementary DNA
CaM	calmodulin
CaMKII	calmodulin-kinase II
CACNA1C	gene of Cav1.2 channel
C-terminus	carboxyl terminus
CMs	cardiomyocytes
DHPs	dihydropyridines
DMEM	Dulbecco´s modified Eagle medium
DMSO	dimethylsulfoxide
DNA	deoxyribonucleic acid
dNTP	2'deoxynucleoside-5'-triphosphate
DTT	dithiothreitol
E18.5	embryonic day 18.5
ECG	electrocardiogram
EDTA	ethylenediamine tetra-acetic acid
EGTA	ethylene-bis(oxyethylenenitrilo)-tetra-acetic acid
FCS	fetal calf serum
FSK	forskolin

g	gram (weight)
	or respective gravity (for centrifugation)
GAPDH	glyceraldehyde-3-phosphate dehydrogenase
glycine	Gly
GTP	guanosine-5'-triphosphate
h	hour
HEK293 cells	human embryonic kidney cells
HEPES	N-2-Hydroxyethylpiperazine-N′-2-ethanesulfonic
HPRT	hypoxanthine phosphoribosyltransferase
HVA	high voltage activated
Hz	hertz
I_{Ba}	current through L-type Ca^{2+} channel using barium as charge carrier
I_{Ca}	L-type Ca^{2+} channel current
IC_{50}	the half maximal inhibitory concentration
IQ motif	isoleucine-glutamine motif
isoproterenol	Iso
isradipine	ISR
kb	kilo base pairs
LTCC	L-type calcium channel
LVA	low voltage activated
Leucine zipper	LZ
M	molar
µM	micromolar
min	minute
ml	millilitre
mM	millimolar
mV	millivolt
N-terminus	amino terminus
nM	nanomolar
OD	optical density

PAAs	phenylalkylamines
PAGE	polyacrylamide gel electrophoresis
pA/pF	picoamperes per picofarad
PBS	phosphate buffered saline
p.c.	post coitum
PCR	polymerase chain reaction
PKA	protein kinase A
PKC	protein kinase C
RNase	ribonuclease
rpm	revolutions per minute
RT	room temperature
RT-PCR	reverse transcriptase polymerase chain reaction
SDS	sodium dodecyl sulfate
sec	second
SEM	standard error of mean
serine	Ser
TEA-Cl	tetraethylammonium cloride
TEMED	N,N,N‘,N‘-Tetramethylethylenediamine
TBS	Tris-buffered saline
Tris	Tris-(hydroxymethyl)-methylamine
U	unit
V	volt
VACCs	voltage-activated Ca^{2+} channels
WT	wild type

Contents

Abbreviations

1. Introduction

Calcium (Ca^{2+}) is a ubiquitous intracellular signaling molecule and serves as a second messenger of electrical signaling (Clapham, 1995; Ghosh *et al.*, 1995). As a major source of Ca^{2+} influx, voltage-activated Ca^{2+} channels (VACCs) fulfill critical roles in Ca^{2+} signaling and are responsible for controlling numerous cellular processes. Especially L-type calcium channels (LTCCs) regulate muscle contraction, hormone secretion, neuronal excitability and gene expression (Berridge *et al.*, 2000; Catterall, 2000b; Clapham, 1995; Dai *et al.*, 2009). For instance, one member of the LTCCs family, the $Ca_V1.2$ calcium channel, is widely expressed and is of functional importance for cardiomyocytes (CMs), smooth muscle and neurons (Catterall, 2000a). Deletion of the $Ca_V1.2$ gene results in cellular disorders; thereby induces a number of diseases. For example, heart specific deletion of the $Ca_V1.2$ channel is embryonically lethal (Seisenberger *et al.*, 2000) and smooth muscle specific deletion of the $Ca_V1.2$ gene leads to intestinal dysfunction (Wegener *et al.*, 2004), defects in blood pressure regulation (Moosmang *et al.*, 2003), even death (Wegener *et al.*, 2006).

1.1. Voltage-activated calcium channels

Voltage-activated calcium channels can be divided into two subclasses based on their electrophysiological and pharmacological properties: low-voltage-activated (LVA) and high-voltage activated (HVA) channels (see Table 1). LVA channels need only a small depolarization to be activated, whereas HVA channels require a relatively high step in membrane voltage to open (Hagiwara *et al.*, 1975; Lacinova, 2005; Llinas *et al.*, 1981). LVA calcium channels were also called T-type calcium channels (T for transient and tiny), because of the small amplitude of single channel conductance, short opening time, fast decay and their activity at more negative membrane potentials; HVA calcium channels contained two subgroups: named L-type calcium channels and neuronal P/Q- N- and R-type channels. L-type calcium channels (L for large and long-lasting), due to their large-single channel conductance amplitude, long opening time, slow kinetics of current decay and their activity at more positive membrane potentials (Lacinova, 2005). A pharmacological hallmark of all L-type calcium channels are their specific inhibition by

Ca^{2+} antagonist drugs including dihydropyridines (DHPs), phenylalkylamines (PAAs) and benzothiazepines (BTZs) (Reuter, 1983). The L-type calcium channels can be further subdivided into 4 subtypes that have been designated as $Ca_V1.1$ (α_{1S}), $Ca_V1.2$ (α_{1C}), $Ca_V1.3$ (α_{1D}) and $Ca_V1.4$ (α_{1F}). $Ca_V1.1$ is mainly expressed in skeletal muscle (De Jongh *et al.*, 1991; Tanabe *et al.*, 1987). $Ca_V1.2$ was detected in several tissues, namely in the heart (Mikami *et al.*, 1989; Striessnig, 1999; Welling *et al.*, 1997), the smooth muscle (Moosmang *et al.*, 2003), the brain (Hell *et al.*, 1993), the pancreas (Schulla *et al.*, 2003) and the adrenal gland (Marcantoni *et al.*, 2007). $Ca_V1.3$ is mainly expressed in the brain, besides it is also found in the heart, kidney, ovary, pancreas and the cochlea (Seino *et al.*, 1992). $Ca_V1.4$ is located in the retina (Strom *et al.*, 1998), the lymphoid tissue and the spinal cord neurons (McRory *et al.*, 2004). The other HVA family contains the P/Q- N- and R-type channels (also know as α_{1A}, α_{1B} and α_{1E}) (Dai *et al.*, 2009). These three types of channels can be activated only by strong depolarization and are not inhibited by the previously mentioned L-type calcium channel antagonists (Catterall, 2000b).

An overview of VACCs known to-date are given in Table 1 and will not be discussed in detail here (Birnbaumer *et al.*, 1994; Dolphin, 2012b; Ertel *et al.*, 2000; Snutch *et al.*, 1990; Tsien *et al.*, 1988).

Table 1: Family of VACCs

	Ca^{2+} current types		Ca^{2+} channels	Gene names
HVA channels		L-type	$Ca_V1.1$ (α_{1S})	*CACNA1S*
			$Ca_V1.2$ (α_{1C})	*CACNA1C*
			$Ca_V1.3$ (α_{1D})	*CACNA1D*
			$Ca_V1.4$ (α_{1F})	*CACNA1F*
	Neuronal	P/Q-type	$Ca_V2.1$ (α_{1A})	*CACNA1A*
		N-type	$Ca_V2.2$ (α_{1B})	*CACNA1B*
		R-type	$Ca_V2.3$ (α_{1E})	*CACNA1E*
LVA channels		T-type	$Ca_V3.1$ (α_{1G})	*CACNA1G*
			$Ca_V3.2$ (α_{1H})	*CACNA1H*
			$Ca_V3.3$ (α_{1I})	*CACNA1I*

1.2. The composition of $Ca_V1.2$ channel

The $Ca_V1.2$ calcium channel, is a multisubunit complex composed of a pore-forming α_1 subunit and auxiliary β, $\alpha_2\delta$ and in some cases γ subunits, e.g., in nerve and skeletal muscle cells (Catterall, 2000b; Ertel *et al.*, 2000; Escayg *et al.*, 2000; Striessnig, 1999). The α_1 subunit is the principal subunit, forming the conduction Ca^{2+} pore and contains a putative selective filter, which ensures high selectivity of the channel pore for calcium ions (Lacinova, 2005). Furthermore, the α_1 subunit undergoes voltage-dependent activation and inactivation, is regulated by second messenger-activated protein phosphorylation pathways and carries the binding sites for blockers and activators (Catterall, 2000b; Striessnig, 1999). The α_1 subunit has four transmembrane domains I-IV; each consisting of six transmembrane segments S1-S6. The fourth segment of each domain serves as a voltage sensor of the channel; the intracellular P-loop connecting the segments 5 and 6 acts as a selectivity filter (Guy *et al.*, 1990) and the interaction site with β subunit is located in the loop between domain I and II (Dai *et al.*, 2009). In addition, the intracellular carboxyl terminus (C-terminus) and amino terminus (N-terminus) of the α_1 subunit may contain various binding sites for regulatory proteins like calmodulin (Dai *et al.*, 2009), influence the current density of the expressed $Ca_V1.2$ channels (Welling *et al.*, 1997) and serve as the signaling platform for channel activity (Catterall *et al.*, 2008).
The remaining subunits, like β , $\alpha_2\delta$ and γ subunits are considered as accessory subunits and play important roles in modulating calcium channel function (De Waard *et al.*, 1996). (1) the intracellular β subunit, if co-expressed *in vitro* with various α_1 subunits, increases peak current (Singer *et al.*, 1991), most likely by facilitating channel pore opening and by increasing the number of channels at the cell membrane (Josephson *et al.*, 1996; Kamp *et al.*, 1996; Neely *et al.*, 1993). (2) the disulfide-linked complex of $\alpha_2\delta$ subunit, besides involved in presynaptic calcium channel abundance and release probability (Hoppa *et al.*, 2012), recently, has been reported to be linked to disease processes (Dolphin, 2012a). (3) the γ subunit, which is mainly expressed in skeletal muscle and brain can modulate current amplitude and inactivation properties (Klugbauer *et al.*, 2000; Letts *et al.*, 1998; Singer *et al.*, 1991).

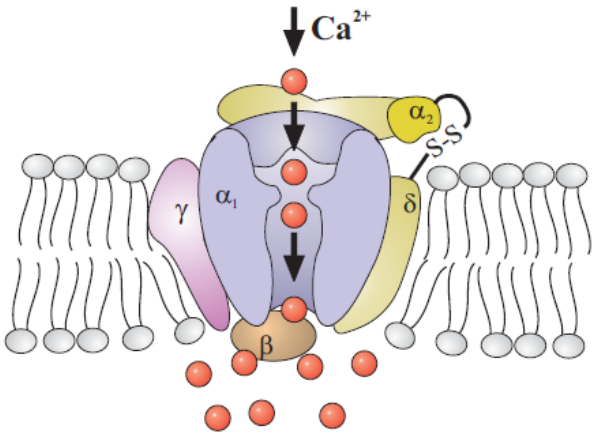

Fig. 1 A proposed schematic structure of $Ca_V1.2$ calcium channel. The principal α_1 subunit is a transmembrane protein containing a conducting pore, through which calcium ions can pass upon opening. α_1 subunit is further regulated by auxiliary subunits: intracellular β subunit, transmembrane γ subunit and a complex of extracellular α_2 subunit and transmembrane δ subunit, connected by a disulphide bridge (Lacinova, 2005)

1.3. The C-terminus of $Ca_V1.2$ channel

The C-terminus of $Ca_V1.2$ contains a plenty of structural elements, including the EF-hand motif, which selectively binds calcium with high affinity (Ozawa, 1995); the isoleucine-glutamine (IQ) motif, which binds the calmodulin (CaM) for both Ca^{2+}-dependent facilitation (CDF) and Ca^{2+}-dependent inactivation (CDI) (DeMaria *et al.*, 2001; Peterson *et al.*, 1999; Van Petegem *et al.*, 2005; Zuhlke *et al.*, 1999; Zuhlke *et al.*, 2000); several phosphorylation sites, such as Ser-1928 phosphorylation site for PKA regulation (De Jongh *et al.*, 1996), Ser-1512 and Ser-1570 phosphorylation sites for CaM-KII facilitated modulation (Blaich *et al.*, 2010; Lee *et al.*, 2006).

Besides, the sequence 1572-1651 in the C-terminal tail of $Ca_V1.2$ determines not only membrane targeting, but also channel inactivation, conductance of single channel and open probability (Kepplinger *et al.*, 2000). In addition, it has been suggested that the C-terminus of the $Ca_V1.2$ contains inhibitory elements, as deletion of parts of the C-terminus results in increased Ca^{2+} current (Wei *et al.*, 1994). Recently, it also has been suggested mutations in amino acid residues 1681-1700 at the proximal C-terminus of $Ca_V1.2$ will influence the efficiency of restoration of action potential-induced Ca^{2+}

transient (Nakada *et al.*, 2012). All in all, a variety of work suggested modifications at the C-terminus of the $Ca_V1.2$ may cause a functional change of the channel.

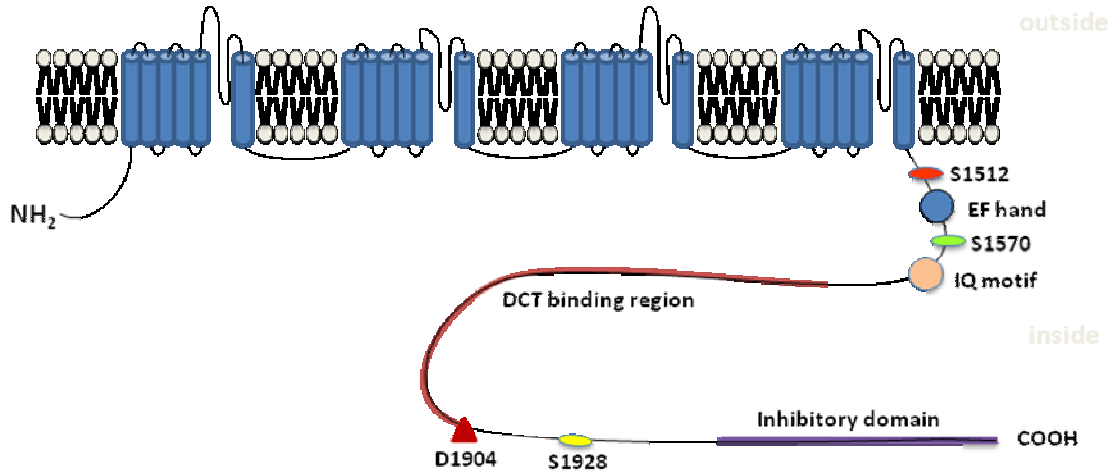

Fig. 2 Suggested structure of the α_1 subunit of $Ca_V1.2$ channel. The α_1 subunit consists of four identical transmembrane domains I-IV, each consisting of six transmembrane segments S1-S6, as well as the two intracellular termini: NH_2 terminus and COOH terminus. The EF-hand, IQ motif and several potential phosphorylation sites are located in the COOH terminus.

1.4. Regulation of $Ca_V1.2$ by PKA in cardiac function

The voltage-gated, L-type calcium channel, $Ca_V1.2$, is the predominantly expressed isoform in cardiomyocytes and mediates excitation-contraction coupling in the heart (Bohn *et al.*, 2000; Ertel *et al.*, 2000; Lipscombe, 2002; Mikami *et al.*, 1989; Seisenberger *et al.*, 2000). The increase in heart rate and contractility during the fight or-flight response is mediated in genereal by *β*-adrenergic receptor stimulation, activates a GTP-binding protein (GS), which stimulates adenylyl cyclase (AC) to produce cyclic AMP (cAMP); cAMP in turn activates protein kinase A (PKA), which is thought to phosphorylate several target proteins including the $Ca_V1.2$ channel, which shows increased current after activation of this cascade (Catterall, 2000b; Fu *et al.*, 2011; Hulme *et al.*, 2003; Osterrieder *et al.*, 1982; Reuter, 1983). It is thought that the interaction of PKA and $Ca_V1.2$ requires A-kinase anchoring proteins (AKAPs) that interact with a leucine zipper (LZ)-like motif within the last 125 residues of intracellular C-terminal segment (Bean *et al.*, 1984; Bers, 2002; Dai *et al.*, 2009; Hulme *et al.*, 2003). To some extent, dysregulation of $Ca_V1.2$, mishandling of cAMP-PKA pathway and thereby Ca^{2+}-induced Ca^{2+} release contributes to the contractile dysfunction and arrhythmias in

pathophysiological conditions (Gomez *et al.*, 1997; He *et al.*, 2001; Pogwizd *et al.*, 2001; Schroder *et al.*, 1998). PKA-dependent phosphorylation signal was found at serine 1928 by several studies, which implied that the intracellular C-terminal tail is the major target of PKA-stimulated phosphorylation mediating the β-adrenergic stimulation of the channel (Fu *et al.*, 2011; Hulme *et al.*, 2006a; Jones *et al.*, 2012). However, Bunemann et al. (Bunemann *et al.*, 1999) reported substantial (greater than twofold) regulation with intracellular perfusion of activated PKA in human embryonic kidney cells co-transfected with $Ca_V1.2$ truncated at 1905 and β_{2a} subunits, which suggested that phosphorylation of serine 478 and/or serine 479 in the β-subunit is required for this regulation. Further the conclusion was confirmed by Gerhardstein BL et al. showing that PKA can not only phosphorylate serine 478 and serine 479 but also serine 459 in the cardiac β_{2a} subunits in cell expression system (Gerhardstein *et al.*, 1999). In contrast to these previous *in vitro* studies, *in vivo* exchange of serine to alanine did not affect the β-adrenergic regulation (Lemke *et al.*, 2008), further confirmed by Brandmayr et al. that both $Ca_V\beta_2$ and Ser-1928 phosphorylation sites were not necessary for β-adrenergic stimulation of the cardiac I_{Ca} (Brandmayr *et al.*, 2012). However, truncation of the $Ca_V1.2$ sequence at Gly-1796 or Aps-1904 leads to loss of β-adrenergic regulation (Domes *et al.*, 2011; Fu *et al.*, 2011). So far, the molecular basis of I_{Ca} regulation by PKA could not be defined conclusively. These findings are in line with the notion that β-adrenergic stimulation of $Ca_V1.2$ channel may require the distal C-terminus but not phosphorylation of serine 1928 (Domes *et al.*, 2011; Ganesan *et al.*, 2006).

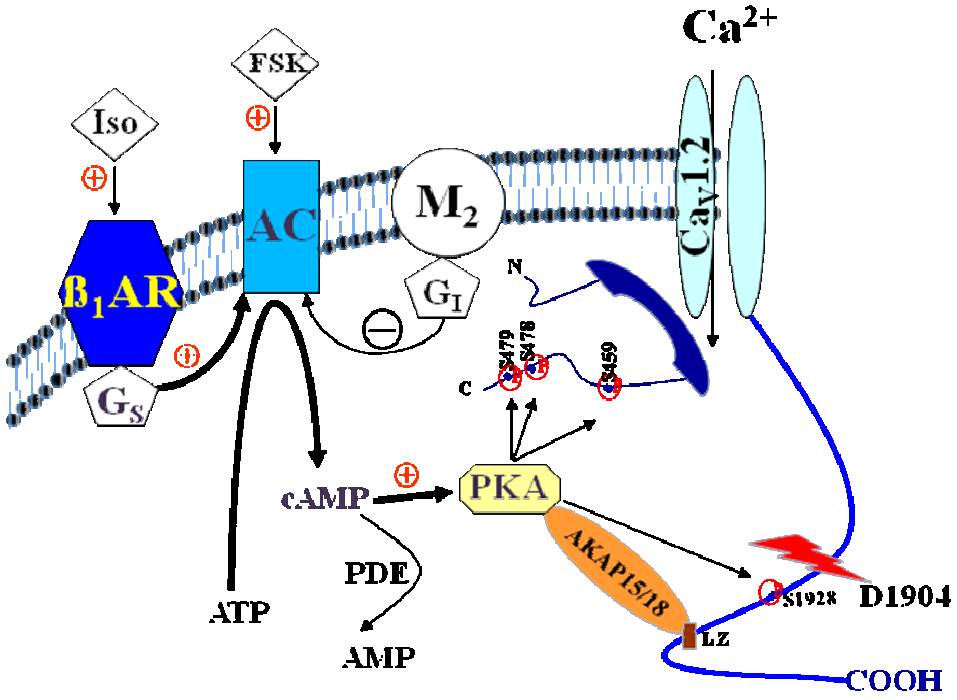

Fig. 3 The regulation of $Ca_V1.2$ channel by the β-adrenergic/cAMP/PKA signaling cascade. The $Ca_V1.2$ channel is regulated by activating of β-adrenergic receptors, adenylyl cyclase, cyclic AMP-dependent protein kinase A (PKA) and then induces phosphorylation at C-terminus of $Ca_V1.2$ in the heart. β-adrenergic regulation of $Ca_V1.2$ channels requires AKAP15/18, which anchors the kinase to distal C-terminus of $Ca_V1.2$ via a modified LZ motif. Arrows indicate the sequence of the β-adrenergic/cAMP/PKA signaling cascade and point to several interaction sites in the C-terminus of α_1 subunit and β subunit.

1.5. Objective of this work

Most studies describing the role of the C-terminus in regulating $Ca_V1.2$ channel activity have been performed in expression systems. In order to further investigate how the truncated $Ca_V1.2$ calcium channel effects *in vivo*, we generated a mouse line that have been inserted three stop codons after aspartate 1904 in murine $Ca_V1.2$ gene, which can prevent the translation of the remaining amino acid residues behind aspartate 1904. Thereafter, we investigated the properties of $Ca_V1.2$ in ventricular and atrial cardiomyocyte from these mice. In parallel, different isoforms and mutants of $Ca_V1.2$ were also examined in HEK293 cells in order to compare the results obtained *in vitro* with those obtained *in vivo*.

2. Materials and Methods

2.1. Chemicals and consumables

All chemicals and consumables used were of molecular biology grade and from Sigma-Aldrich, Carl Roth, Sarstedt, Biochrom and Merck unless otherwise indicated. All solutions were prepared with ultra-pure water (Millipore, Molsheim, France) and were autoclaved or sterilized with a 0.2 µm syringe filter unless otherwise specified. They were stored at 4°C and pre-warmed to 37°C prior to use. The composition of specific solutions is given in the relevant methods.

Reagent	**Source**
Agarose	Biozym
BC Assay Protein Quantification Kit	interchim®
Bortezomib	LC Laboratories
Bovine serum albumin	GibcoBRL
DMEM	Invitrogen
ECL Advanced Western Blot Detection Kit	GE Healthcare
fetal calf serum	Gibco
Lactacystin	Calbiochem
Liberase DH	Roche Applied Science
Lipofectamine™ 2000	Invitrogen
MG132	Calbiochem
OptiMEM	Gibco
Penicillin/Streptomycin 100x	Gibco
peqGOLD RNA Pure Kit	Peqlab
Plasmid Maxi Kit	Qiagen
Quantum 286 Medium	PAA
RNeasy Plus Micro Kit	QIAGEN
Standardmarker DNA-Extension-ladder	Gibco
Standard marker Precision Blue Protein Standard	Gibco
Trypsin/EDTA 10x	Gibco

2.2. Devices

Device	Manufacturer
4°C Refrigerator	Liebherr
-20°C Freezer	AEG
-86°C Freezer HERAfreeze	Thermo Fisher Scientific
Agarosegel chamber	MWG Biotech
Axonpatch 200B	Molecular Devices
Biological Safety Cabinets	NuAire
Dark Hood DH-40/50	biostep®
Digidata 1322A digitizer	Molecular Devices
DMZ-Universal Puller	Dagan
Eppendorf Centrifuge 5804R	Eppendorf
Eppendorf Centrifuge 5417R	Eppendorf
Eppendorf Centrifuge 5415C	Eppendorf
Incubator Binder CB53	Binder
Microscope Stemi SV6	Zeiss
Microscope Axioscope	Zeiss
Micro Forge MF-830	Narishige
NanoDrop ND-1000	Peqlab
Oven 37°C	Memmert
PCR-Machine Biometra T Gradient	Biometra
pH-Meter 766 Calimatic	Knick
Semi-Dry-Blotter Maxi	Carl Roth
Standard Power Pack P25	Biometra
Tabletop centrifuge	Neolab
Thermomixer Compact	Eppendorf
Vacuum Concentrator	Bachofer
Vortex-Mixer	NeoLab
Waterbath MT/2	Mgw Lauda

2.3. Cell biological methods

2.3.1. HEK293 cells culture

Human embryonic kidney cell (HEK293 cell) expression system was used for transfection experiment. The cells were cultured in Quantum 286 medium with 100 U penicillin & 100 g/ml streptomycin (penicillin/streptomycin), and then incubated at 37°C and 5.5% CO_2. The cells were passaged once they approached confluence. Quantum 286 medium was removed and cells were washed two times with PBS. Afterwards, cells were predigested with Trypsin/EDTA (2 ml per 75-cm^2 cell culture flask) at room temperature (RT) to allow detachment of the cells from the bottom of cell culture flask (TPP, Trasadingen, Switzerland, 75 cm^2). The added 8 ml Quantum 286 medium will terminate the digestion of Trypsin/EDTA. The cells were further separated by repeated pipetting up and down. If the cell density was to be determined, 50 µl of the cell suspension was dropped on a Neubauer couting chamber and the cell numbers were counted in four 0.1-mm^3 chambers under binocular microscope. The required cell concentration was adjusted by diluting the cell suspension with fresh Quantum 286 medium in 24-well cell culture plate (20000 cells per well) and (20% - 30% confluent). Finally, the cells were seeded back in appropriate density (20% - 30% confluent) with penicillin/streptomycin in 75-cm^2 cell culture flask and part of cells was cultured in 24-well cell culture plate (20000 cells/well).

1 x PBS buffer

NaCl	40 g
Na_2HPO_4 $2H_2O$	3.9 g
KCl	1 g
KH_2PO_4	1 g
H_2O	Ad 5000 ml

pH 7.4 autoclave

Trypsin/EDTA

10 ml trypsin solution stock (0.5% trypsin/0.2% EDTA)	
PBS	Ad 90 ml
pH 7.4	

2.3.2. Freezing, storage and thawing of HEK293 cells

For storage confluent cells from flask, cells were trypsinized and the detached cells were centrifuged at 500 g for 5 min. The pellet was resuspended in 3 ml freezing medium, which contains fetal calf serum (FCS) + 10% dimethylsulfoxide (DMSO). The cell aliquots (1 ml) were first frozen in cryovials at -80°C overnight before transferred to liquid nitrogen for long time storage. For thawing, cryopreserved cells were slowly warmed at RT, transferred to new flask with 20 ml pre-warmed Quantum 286 medium, then incubated at 37°C and 5.5% CO_2 overnight. Next day, incubated in another 20 ml fresh Quantum 286 medium with 200 µl penicillin/streptomycin.

2.3.3. Transfection of HEK293 cells

For transfection of HEK293 cells, Lipofectamine™ 2000 (mixture of cationic and neutral lipids) was used (Lee *et al.*, 2006). For following electrophysiological experiments, we seeded the HEK293 cells on poly-(L)-lysine treated glas cover slips (coat for 1 h with poly-(L)-lysine) which needed to be placed into each well. We seeded 20000 cells per well into 24-well cell culture plate with supplemented Quantum 286 medium to 1 ml. an incubated at 37°C and 5.5% CO_2 for 24 h. Cells should be 80% - 85% confluent before transfection. Next day, HEK293 cells stably expressing $Ca_V a_{1C}$, $Ca_V \beta_{2a}$ and $Ca_V \alpha_2 \delta$ subunits (0.15 µg of each) were transiently transfected using Lipofectamine™ 2000 according to the manufacturer's guide (Invitrogen).

Transfetion mix (per well) and process for electrophysiological experiments	
Solution A	Solution B
0.15 µg DNA	0.5 µl Lipofectamine 2000
Add 50 µl OptiMEM	Add 50 µl OptiMEM

	Incubate 5 min at RT
Mix gently and incubate 20 min at RT	
Add 100 µl transfection mix to each well; mix gently by moving whole well-plate	

After transfection, the cells were grown for 24 - 48 h at 37°C and 6% CO_2 before beginning the electrophysiological experiments. Exchange the Quantum 286 medium after 24 h against OptiMEM (GIBCO).

For following Western blot experiments, cells were cultured in flask (75 mm^2) in Quantum 286 medium, until they had grown to about 80% - 85% confluent before transfection. Use the 24-well plate protocol with the following modifications:

Transfetion mix (per well) and process for Western blot experiments	
Solution A	Solution B
10 µg DNA	33.3 µl Lipofectamine 2000
Add 3.3 ml OptiMEM	Add 3.3 µl OptiMEM
	Incubate 5 min at RT
Mix gently and incubate 20 min at RT	
Add transfection mix to 75mm2 flask; mix gently by moving whole flask	

The flask was added 20 ml OptiMEM to final volume and incubated for 24 - 48 h at 37°C and 6% CO_2 before beginning the Western blot experiments.

2.3.4. Isolation and primary culture of murine embryonic cardiomyocytes

Individual embryos were obtained after breeding of heterozygous mice. The parents were mated in the evening. Next morning a plug-check was carried out and the plug-positive females were separated. For pregnancy mice this morning were counted as "day 0.5". At embryonic day 18.5 (E18.5), heterozygous pregnant mice were killed by cervical dislocation, and the uterus was removed and placed in 37°C pre-warmed ADS buffer. The uterus was rinsed once and opened longitudinally to expose the embryos still contained within the decidua. Embryos were dissected from the uterus as described

(Seisenberger *et al.*, 2000). Briefly, after placing the embryos in ADS buffer, the heart was removed from the embryo. The atrium and ventricle can be distinguished by localization and color and were separated, respectively. A piece of tail sample from embryos was also kept for later gentyping identification. The tissue was placed in an (1.5 ml) Eppendorf tube filled with 0.5 ml ADS buffer and spun briefly to replace the solution with fresh ADS buffer containing 0.25 mg/mL Liberase DH (Roche Applied Science) dissolved in 0.5 ml ADS buffer. Digestion was allowed for 15 minutes at 37°C, 400 rpm in Thermomixer compact shaker (eppendorf) by gentle trituration of the tissue. Thereafter, 0.5 ml of Dulbecco's modified Eagle's medium (DMEM) supplemented with 5% FCS and penicillin/streptomycin was added to each well to terminate the digestion. After repeated pipetting up and down, the atria and ventricles were gently resuspended and the undigested portion was precipitated to the bottom after 5min incubation. 300 ul supernatant was pipetted on plastic cover slips into each well filled with 1.5 ml DMEM supplemented with 5% FCS and penicillin/streptomycin. Then, the cells were incubated for at least 24 h at 37°C and 10% CO_2. Electrophysiological recordings were made at least 24 h after plating. Analysis for genotyping was performed by PCR.

ADS buffer (mMol/L)

NaCl	116
NaH_2PO_4	1
KCl	5
$MgSO_4$	0.8
HEPES	20
Glucose	5.5

pH 7.35 autoclave

2.4. Whole-cell mode patch champ electrophysiological recordings

The functions of the single or multiple ion channels in cell membranes can be studied, with the development of patch-clamp technology (Hamill *et al.*, 1981; Neher *et al.*, 1992). In our study, the whole-cell configuration of the patch clamp technique was used to record current through L-type calcium channel in transfected HEK293 cells and

embryonic cardiomyocytes isolated at E18.5 using barium as the charge carrier (I_{Ba}). Stimulation and data acquisition were performed by Axonpatch 200B (www.moleculardevices.com) with a Digidata 1322A digitizer and the Pclamp 9 software package (all from Axon Instruments). Data were sampled at 5 kHz and filtered at 1 kHz. The patch pipettes were made from borosilicate glass capillaries and were pulled by microelectrode puller (DMZ-Universal Puller) and further fire-polished (MF-830, Narishige Japan) before use. The input resistance of the patch pipettes ranged from 1.5 to 2 MΩ when filled with intracellular solution. The patch pipette was brought to the cell surface, and then sucked the membrane gently into the pipette to generate gigaseal. Applying strong suction to achieve whole-cell recording mode on ruptured the cell membrane. Thereafter, the current through the channels in the membrane will be recorded. Series resistance and capacitive components were not compensated. The composion of internal solution and external solution used for HEK293 cells or embryonic cardiomyocytes were showed below. Peak Ba^{2+} current amplitude was plotted *versus* voltage to generate current-voltage (I-V) relationship. Holding at -80 mV, the cell was stimulated with 300 ms square pulses from -40 to +60 mV in increments of 10 mV at 0.2 Hz. A pre-pulse from -80 to -40 mV was applied for 25 ms to inactivate fast sodium current. Current was measured as the difference between the peak current during depolarization and the base line at -80 mV. All experiments were performed at room temperature.

External solution (mMol/L) for HEK293 cells and CMs

NaCl	82
TEA-Cl	20
$BaCl_2$	30
CsCl	5
$MgCl_2$	1
EGTA	0.1
glucose	10
HEPES	10

pH 7.4 adjusted with NaOH

Internal solution (mMol/L) for HEK293 cells

CsCl	102
TEA-Cl	10
EGTA	10
$MgCl_2$	1
Na_2ATP	3
HEPES	5

pH 7.4 adjusted with CsOH

Internal solution (mMol/L) for CMs

CsCl	60
aspartic acid	50
CsOH	68
$MgCl_2$	1
Na_2ATP	5
HEPES	10
EGTA	10

pH 7.4 adjusted with CsOH

2.5. Biochemical methods

2.5.1. Protein production by SDS/Tris-digestion

2.5.1.1. Protein production from murine tissues

The tissues were isolateded from the murine embryos at day E18.5 and immediately frozen in liquid nitrogen. Subsequently, the frozen tissues were pulverized in a -20°C pre-cooled mortar on dry ice. The homogenized powder was mixed with 2% sodium dodecyl sulfate (SDS)/50 mM Tris-(hydroxymethyl)-methylamine (Tris), pH 7.4 (100 µl/10 mg tissue), and heated for 15 min at 95°C with occasional vortexing, then centrifuged at 20000x g for 5 min. Subsequently, the supernatant was aliquoted and frozen at -80°C.

2.5.1.2. Protein production from HEK293 cells

For the SDS-digestion, the cultured HEK293 cells in 25 mm^2-flask were washed with PBS and collected in a 15 ml-Falcon, then centrifuged at 5000 g for 5 min mix in 250 µl 2% SDS/50 mM Tris, pH 7.4, without supernatant. The mixture was then transferred into a 1.5 ml reaction vessel and heated for 15 min at 95°C with occasional vortexing, centrifuged for 5 min at 20000x g. Subsequently, the supernatant was aliquoted and frozen at -80°C.

2.5.2. Quantitative protein determination

To estimate the protein content, the BC Assay Protein Quantification Kit (interchim®) was used. This test is based on a redox reaction: it involves the reduction of Cu^{2+} to Cu^{+} by proteins in an alkaline medium, and then Cu^{+} ions are chelated by with BC Assay (bicinchoninic acid) to form a water soluble purple coloured complex, which shows a strong absorption at 540 nm. Bovine serum albumin (BSA) (GibcoBRL) standards were prepared from concentrations of 100 to 1000 mg/ml in water. 200 µl of a mixture of BC Assay Reagent A and B mixed (50:1) standard solution was added to 50 µl of BSA standard or diluted protein sample. The mix solution was incubated for 45 - 60 min at 60°C in a thermo shaker and transferred to a 96-well plate. The absorbance was determined at 540 nm using H_2O as a blank value (Multiskan MCC/340), then a calibration curve of the protein concentration versus absorbance was obtained and protein sample concentration was calculated.

2.5.3. Electrophoretic separation of proteins by SDS-PAGE

Electrophoretic separation of proteins according to their molecular weight was carried out by anionic detergent SDS-polyacrylamide gel electrophoresis (PAGE). The anionic detergent can bind to the proteins and forms micelles. By the SDS micelles are negatively charged and migrate in an electric field to the anode, enable separation according to the molecular weight of the proteins. Resolving gel solution was prepared according to the protocol as follows and poured between two glass plates (Biorad), 1.5 cm below the

lower edge, then overlaid with 100% ethanol to provide a smooth surface. After completing the polymerization (about 30 min after adding APS and TEMED), the ethanol was removed and the top of gel was washed with water for 3 times. After removing all residual liquid the freshly prepared stacking gel solution was filled and immediately set a gel comb in the stacking gel. This generated gaps which the samples can be given later. Subsequently the gel was placed in Mini-Protean Tetra System gel chamber (Biorad) filled with 1×electrophorese buffer. For electrophoresis 4x Lamemmli buffer containing DTT was added to the samples. The protein samples and a protein standard were loaded onto the SDS-PAGE gel. Then a voltage of 60 V was initially applied untill the running front passed into the resolving gel, thereafter the voltage was increased to 150 volts. The resolving gel was subjected to Western blot analysis

4 x Tris/SDS pH 6.8 (Stacking gel)

Tris Base	6.04 g
SDS	0.4 g
H_2O	Ad 1000 ml

4 x Tris/SDS pH 8.8 (Resolving gel)

Tris Base	18.2 g
SDS	0.4 g
H_2O	Ad 1000 ml

10 x Electrophorese buffer

Tris Base	30.2 g
Glycin	144 g
SDS	10 g
H_2O	Ad 1000 ml

4 x Lamemmli buffer

1M Tris (pH 6.7)	10 ml
20% SDS	12.5 ml

Bromphenolblau	20 mg
Glycerin	20 ml
DTT	2 mg
H_2O	Ad 50 ml

Stacking gel

29:1 Acrylamide	325 µl
4 x Tris/SDS (pH 6.8)	625 µl
H_2O	1525 µl
APS	6.25 µl
TEMED	2.5 µl

Resolving gel

	6%	7.5%	8%	10%	
29:1 Acrylamide	3.0	3.75	4.0	6.0	ml
4 x Tris/SDS (pH 8.8)	3.75	3.75	3.75	3.75	ml
H_2O	8.25	7.50	7.25	6.25	ml
APS	50	50	50	50	µl
TEMED	10	10	10	10	µl

2.5.4. Western blot analysis

This part was performed by Dr. Katrin Domes. After electrophoresis proteins were transferred to a special PVDF membrane (Immobilon-P, Millipore) on which they can be detected using specific antibodies (Burnette, 1981; Towbin *et al.*, 1979). The PVDF membrane and 10 electrode papers (Whatman 3MM) were cut as the size of the polyacrylamide gel. The PVDF membrane was placed onto the gel and both were sanwiched between electrode papers (three of electrode papers were soaked in anode buffer 1; two of them were soaked in anode buffer 2 and 5 of them were soaked in cathode buffer and the membrane was soaked briefly in methanol then rinsed in anode buffer 2), then this stack was placed on the anode plate, covered with the cathode plate.

Next we applied 0.8 mA/cm^2 current for one hour to transfer the proteins to the membrane in ice-cold transfer buffer. None-specific binding sites on the blotted membrane were blocked in blocking solution (5% milk powder in 1x TBST) and incubated overnight at 4°C. Next day, the membrane was washed two times in 1x TBST for 15 min before incubation with the primary antibodies. After incubation with the primary antibodies for 90 min at room temperature, the immublots were washed three times with 1% milk powder in 1x TBST for 10 min. The immunoblots were then incubated with appropriate secondary antibody for 1 h at room temperature (see Table 2). It was followed by a further washing step (twice for 10 min with 1% milk powder in 1x TBST, twice for 5 min in 1x TBST) before the immunoblots were visualized by the ECL Advance Western Blotting Detection Kit (GE Healthercare) and the films were detected by the CCD camera of the LAS4000 mini and evaluated with the Multi Gauge 2.0 software.

10 x TBS (pH 8.2)

Tris Base	12.1 g
NaCl	87.5 g
H_2O	Ad 1000 ml

1 x TBST

10 x TBS	100 ml
NaCl	87.5 g
H_2O	Ad 1000 ml

Table 2: Antibody used to Western blot analysis

Primary Antibodies			
Antibody	Origin	Dilution	Reference
$Ca_V1.2$	Polyclonal rabbit	1:250	Institute of Pharmacology and Toxicology, TUM (Domes *et al.*, 2011; Moosmang *et al.*, 2003)

GAPDH	Polyclonal rabbit	1:5000	Sigma
α-actinin	Monoclonal mouse	1:5000	Sigma

Secondary Antibodies			
Antibody	Origin	Dilution	Reference
Anti-rabbit (peroxidase-coupled)	Goat	1:50000	Dianova
Anti-mouse	Goat	1:5000	Dianova

2.5.5. Animals

All experiments were performed on mice which were maintained and bred in the animal facility of the institute of Pharmakology and Toxicology, Technical University of Munich and had access to water and standard chow ad libitum. All procedures relating to animal care and treatment conformed to the institutional and governmental guidelines of Bavaria (Germany).

2.5.6. Generation of Cav1.2$^{D1904Stop/D1904Stop}$ mice

This part was performed by Dr. Toni Lemke. A 7.4 kb fragment containing exons 44 - 47 of *CACNA1C* was isolated from 129/Sv mouse genomic DNA for constructing the targeting vector. A 1.2 kb short arm and 6.2 kb long arm with PGK-neo and the thymidine kinase gene (tk) flanked by two loxP sites comprised the targeting vector. The 5′-side short arm contained exon 44 with three stop codons (TGA TAA TAG) inserted after the base triplet corresponding to aspartate 1904. All mutation procedures were carried out by overlap PCR mutagenesis. The targeting construct was electroporated into R1 ES cells (129/Sv × 129/Sv-CP F1). Positive clones were identified by polymerase chain reaction and confirmed by Southern blot using an outer probe (5'-probe in Figure 1A). In order to delete the neo/tk marker genes, two positive clones were transfected with a Cre-expressing plasmid. Three clones with the deletion event were injected in C57BL/6 blastocysts, and chimeras were crossed to C57BL/6 mice. Heterozygous mice were bred to produce homozygotes. We used 129/Sv and C57BL/6 hybrid genetic background (Cav1.21904Stop-129B6F2) for all analysis (Domes *et al.*, 2011).

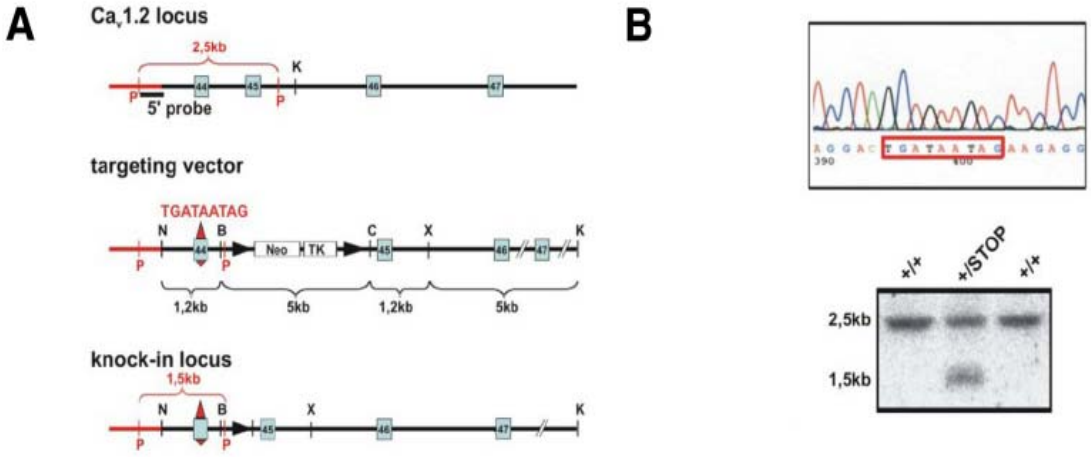

Fig.4 Generation of Cav1.2$^{D1904Stop/D1904Stop}$ mice. A, top panel: genomic DNA structure of *CACNA1C* with the relevant restriction enzyme sites; boxes represent exons 44 - 47 encoding the C-terminus of $Ca_V1.2$. Middle panel, targeting vector. Neo, neomycin resistance gene; TK, thymidine kinase gene with the loxP sequence (triangles) at both sides. The insertion of the three stop codons after aspartate 1904 is shown. Bottom panel, knock-in locus after homologous recombination and Cre-mediated deletion of resistance markers. The 5' probe, which contains genomic sequence outside of the targeting vector, is depicted as a solid bar. K, KpnI; N, NotI; B, BamHI; C, ClaI; X, XhoI; P, PstI; kb, kilobases. B, top panel: sequence analysis of genomic DNA in the region coding for Asp-1904 from Cav1.2 asp1904Stop/asp1904Stop mice. Bottom panel: Southern blot using the 5' probe. Wild type (+/+) and heterozygote (+/Stop) sequence are indicated.

2.5.7. Construction of Cav1.2 cDNA

C-terminal truncated constructs were generated using Quick change mutagenesis (Stratagene) by inserting a single stop codon (TGA) after the amino acid 1905 in rabbit corresponding to mouse 1904 in pcDNA3 vectors (Invitrogen). Cav1.2 cDNAs used were rabbit heart (HK; accession number: X15539) and smooth muscle (LK; accession number: X55763). All constructs were verified by double strand sequencing (Domes *et al.*, 2011).

2.6. Molecular biological methods

2.6.1. Genotyping identification by polymerase chain reaction (PCR)

Specific DNA segments can be amplified by PCR. Primers were commercially synthesized (Eurofins MWG Operon). They were designed corresponding to the DNA segment to be amplified.

Table 3: Primers used to identify genotyping (for, forward primer; rev, reverse primer)

Primer	Sequence	Mouse line
Primer_for	5' GAC CCT TGT GTA GAG AGT GAG CC 3'	$Ca_V1.2^{Stop}$
Primer_rev	5' CAA AAG TAG CCG GGG AAC CG 3'	$Ca_V1.2^{Stop}$

Reaction parameters for DNA amplification (for, forward primer; rev, reverse primer)

Template DNA	10-500 ng (except in negative control PCR)
PCR reaction buffer 1x	7 µl
Primer_for (25 µM)	0.3 µl
Primer_rev (25 µM)	0.3 µl
GoTag Polemerase (1.5 U)	0.3 µl
H_2O	ad 25 µl

PCR reaction buffer 1x

dNTPs (10 mM)	50 µl
$MgCl_2$	150 µl
5x Green GoTag Flixi buffer	500 µl
Aliquot and freeze at 20°C	

Thermal cycle paramenters for PCR

94°C (Initial denaturation)	5 min	
94°C (Denaturation)	30 sec	}
58°C (Primer annealing)	30 sec	}
72°C (Elongation)	1 min	}
72°C	10 min	

The annealing temperature was varied according to the melting temperature of the primers. Elongation time depended on the length of the desired product, with 1 min used for amplifaction of 1 kb.

2.6.2. RNA applications

2.6.2.1. RNA isolation and quantification

Frozen ventricular and atrial tissues were homogenized in lysate buffer and total RNA was isolated by using RNeasy Plus Micro Kit (QIAGEN) according to the manufacturer's recommendations. Total RNA was quantified by spectrophotometer (Nanodrop 2000, Thermo Scientific). The concentration of RNA was photometrically measured at 260 nm and one OD260 corresponded to 40 µg/ml for RNA. The A260/A280-ratio of absorbance at 260 and 280 nm was used to assess the purity of RNA. A ratio of ~2.0 is generally accepted as "pure" for RNA. Then the RNA samples were stored at -80°C.

2.6.2.2. First strand cDNA synthesis

First strand cDNA synthesis was carried out using Superscript II reverse transcriptase (Invitrogen) according to the manufacturer's recommendations. A reaction mixture contained 1 ng ~ 5 µg of total template RNA, Oligo-dT primer, 10 mM dNTP Mix, 0.1 M DTT, 1.5 units of Rnase H, 5× first strand buffer and 200 units of Superscript II reverse transcriptase. The enzyme was inactivated by incubating at 90°C for 5 min. The cDNAs were first analyzed with a GAPDH or HPRT-specific as an internal control. Specific primer pairs were used to detect Cav1.2a, Cav1.2b, $Ca_V1.3$ and Cav2.1 transcripts (Table 3). 10 µl template RNA (unless this exceeds or undercuts the required 1 ng - 5 µg amount of RNA) and 1 µl Oligo-dT primer (0.5 µg) were mixed to a final volume of 11 µl and incubated for 10 min at 70°C. 4 µl 5×first strand buffer, 2 µl DTT (0.1 M) and 1 ul dNTPs (10 mM) were added and the solution was incubated for 2 min at 42°C. The reverse transcriptase was then supplemented and the mixture was incubated for 1 h at 42°C. Superscript II (200 units) reverse transcriptase was heat-inactivated for 5 min at

90°C. Rnase H (1.5 units) was finally added to destroy RNA leftovers and the total solution was incubated for 20 min at 37°C. Total strand cDNA samples were then quantified by spectrophotometer. The concentration of cDNA was photometrically measured at 260 nm and one OD260 corresponded to 33 µg/ml for single-stranded cDNA. The A260/A280-ratio of absorbance at 260 and 280 nm was used to assess the purity of DNA. A ratio of ~1.8 is generally accepted as "pure" for DNA.Then the first strand cDNA samples were stored at -20°C.

2.6.2.3. Gene expression analysis at the mRNA level using RT-PCR

For gene expression analysis, first strand cDNA was subjected to PCR in order to amplify cDNA fragments derived from expressed target gene-specific mRNA transcripts. The cDNAs were first analyzed with a GAPDH or HPRT-specific as an internal control. Specific primer pairs were used to detect Cav1.2a, Cav1.2b, Cav1.3 and Cav2.1 transcripts (see Table 3). For each primer pair, amplification of the cDNA was carried out in a reaction mixture containing 1 ~ 2 µl of the first strand cDNA preparation, 1× PCR buffer, 3.75 ~ 10 pmol of each primer and 1.5 units of *Taq* polymerase (Promega) in a total volume of 25 µl. The PCR cycles were denaturing at 94 °C for 30 sec, annealing at appropriate temperature for 30 sec and extending at 72°C for 1 min during 30 ~ 35 cycles. The PCR products were separated on 2% agarose gels and stained with ethidium bromide. The gels were recorded and analyzed by imaging software (www.ezquant.com). The relative amount of the amplicons were determined and normalized to that of the GAPDH or HPRT fragment. The identity of the PCR products was verified by DNA sequencing.

Table 4: Primers used to amplify the calcium channel cDNAs and the predicted product size (for, forward primer; rev, reverse primer)

Name	Sequence	Size (bp)
$Ca_V1.2a$_for	5'-ATGATTCGGGCCTTTGTTCAG-3'	228
$Ca_V1.2a$_rev	5'-TGGAGTAGGGATGTGCTCG-3'	

$Ca_V1.2b$_for	5'-ATGGTCAATGAAAACACGAGG-3'	137
$Ca_V1.2b$_rev	5'-TGGAGTAGGGATGTGCTCG-3'	
$Ca_V1.3$_for	5'-TGAAGGAGAAGATTGCGCCC-3'	189
$Ca_V1.3$_rev	5'-TTGCGGAATGAGTGGCTACG-3'	
$Ca_V2.1$_for	5'-CACCAACCCTGGTCCCGCCT-3'	333
$Ca_V2.1$_rev	5'-CATGGGCTTTGGGCCGTCCT-3'	
GAPDH_for	5'-CGGCAAATTCAACGGCACAGTCA-3'	596
GAPDH_rev	5'-GGTTTCTCCAGGCGGCACGTCA-3'	
HPRT_for	5'-GTAATGATCAGTCAACGGGGGAC-3'	175
HPRT_rev	5'-CCAGCAAGCTTGCAACCTTAACCA-3'	

2.7. *In vivo* investigations

This part was performed by Dr. Katrin Domes.

2.7.1. Measurement of cardiac force development

The cardiac ventricles of new born mice were threaded onto sewing silk and fixed in organ baths containing Tyrode's solution (mM) (5.4 KCl, 1 $MgCl_2$, 137 NaCl, 1.8 $CaCl_2$, 5.6 Glucose, 12 $NaHCO_3$, 0.42 NaH_2PO_4) gassed with carbogene. Contraction ability was measured with DMT Multi wire myograph system (model 610M) and recorded with Chart5 for Windows (ADInstruments, Germany) (Domes *et al.*, 2011).

2.7.2. ECG Recordings

Radiotelemetric ECG transmitters ETA-F20 (DSI, St. Paul, MN) were attached to the new born babies. The ECG leads were bonded onto left chest muscle and the right hind limb. Data were acquired using the DSI acquisition system (Domes *et al.*, 2011).

2.8. Statistical analysis

Data plotting and statistical analysis were carried out using ORIGIN software (version 6.1052, Microcal, Northampton, MA). Values given as means ± SEM. Statistical significance was calculated by the Student's *t* test, ANOVA or 2-way ANOVA followed

by Bonferroni post-test. Significant differences are indicated by *, $p < 0.05$; **, $p < 0.01$; and ***, $p < 0.001$.

3. Results

3.1. Functional analysis of cardiac activity in Stop/Stop mice

The functional analysis of cardiac activity was performed by Dr. Katrin Domes.

3.1.1 Breeding of Stop/Stop mice

Heterozygous WT/Stop mice were used to breed Stop/Stop mice. The resulting offsprings were analyzed for their genotype at postnatal day 7 (D7). Unfortunately, Stop/Stop mice were not included in the offsprings although they were expected to be present at a 25% ratio according to Mendel's law (Fig. 5). Consequently, the unborn embryos were analyzed for their genotype at embryonic day 18.5 (E18.5). At this date, 315 embryos from a total of 32 pregnant females followed a Mendelian ratio in the genotype distribution and Stop/Stop mice were found to be present at the expected 25% ratio (Fig. 5). This result shows that the Stop mutation in the $Ca_V1.2$ gene is lethal for the embryos around and/or after birth indicating that the intact Cav1.2 channel is essential for normal development of the embryo.

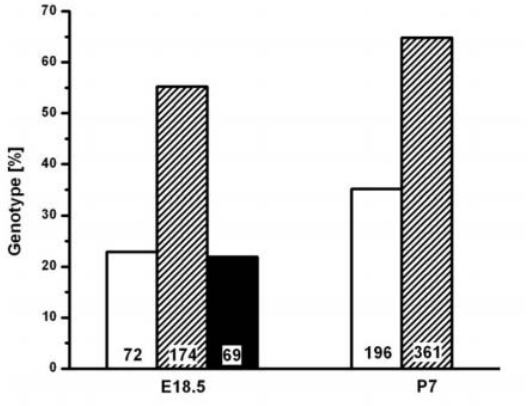

Fig. 5 Distribution of WT, WT/Stop and Stop/Stop embryos at day E18.5 and newborns at postnatal day 7. The numbers of embryos/newborns analyzed are showed in the columns. Genotype was analyzed by PCR.

3.1.2. Paraffin sections of the heart

It has been reported previously that hearts from mice in which the $Ca_V1.2$ channel was truncated at Gly-1796 developed right ventricular hypertrophy, which caused pooling of blood in internal organs (Fu *et al.*, 2011). To investigate whether or not truncation at Asp-1904 induces hypertrophy, the histological studies of the embryonic hearts and the paraffin sections were made at day E18.5. After a Masson trichrome Staining, ventricular perimeter and septum diameter were measured using digitization with a Zeiss AxioCam. As Fig. 6A shows ventricular perimeter of Stop hearts and wild-type hearts (WT hearts) were 6.91 ± 0.16 mm and 6.67 ± 0.13 mm, respectively. The septum diameter of Stop hearts (0.40 ± 0.01 mm) and WT hearts (0.44 ± 0.02 mm) were also very similar (Fig. 6B). These results mean that E18.5 Stop hearts expressing the Cav1.2 channel truncated at Asp-1904 have an unaltered cardiac size (Fig. 6A) and normal septum thickness (Fig. 6B) as compared with WT hearts, indicative of normal blood pressure during feto- and embryogenesis.

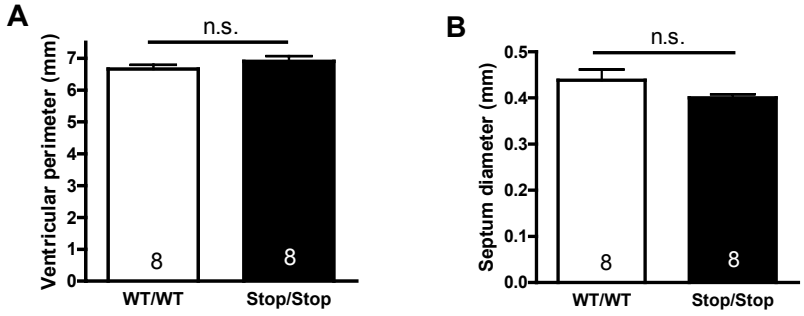

Fig. 6 A, cardiac circumferences were measured in paraffin section of E18.5 hearts. B, the thickness of the cardiac septum was measured in paraffin section of E18.5 hearts. The number of embryos/animals analyzed is showed in the columns. Genotype was analyzed by PCR. Columns represent means ± SEM with n = 8. n.s., not significantly different.

3.1.3. Measurement of electrocardiogram and cardiac contractility

Electrocardiogram (ECG) and cardiac contractility of pups delivered by cesarean section at day E18.5 were examined to investigate the cause of the premature death of the Stop/Stop mice. As we can see from the ECG traces in Fig. 7A, the Stop pups developed arrhythmia after birth, whereas no arrhythmia was observed in WT pups. The heart rates

of the Stop pups were also determined from the ECG trace. As Fig. 7B shows, the heart rates of Stop pups were 124.8 ± 27.7 beats per minute, which were significantly lower than those of the WT, 295.0 ± 33.9 beats per minute. The heart rates of heterozygous pups were 309.9 ± 14.6 beats per minute, with no significant difference from the WT pups.

The force of contraction (*Fc*) was severely reduced by about 50% in the ventricular muscle of the Stop (2.7 ± 0.3 mN) compared with the WT (Fig. 3C and D), but no difference was observed between the WT (5.3 ± 0.8 mN) and heterozygotes (5.5 ± 0.5 mN). All these measurements were performed by a blinded experimentaor. Thereafter, the genotype of the pups was determined by PCR. These findings suggest that failure of up-regulating the beating frequency and reduced *Fc* maybe relative to the dysfunction of truncated $Ca_V1.2$ channel.

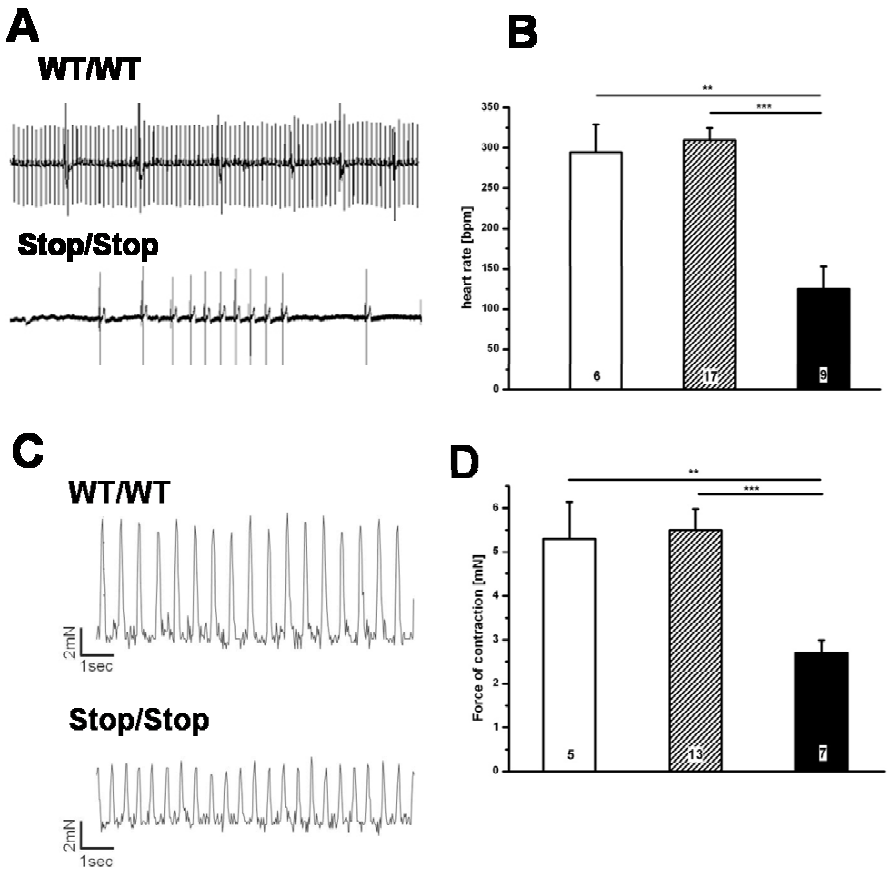

Fig.7 A, electrocardiograms of a WT (upper trace) and a Stop/Stop (lower trace) pup delivered by Cesarean section at day E18.5. B, heart rate of WT, WT/Stop and Stop/Stop pups delivered by Cesarean section at day E18.5. Heart rate (bpm) was determined by ECG recording. C, traces of force development of a WT (upper trace) and a Stop/Stop (lower trace) heart from pup delivered by Cesarean section at day E18.5. D, force of contraction in mN of WT, WT/Stop and Stop/Stop hearts of pups delivered by cesarean section at day E18.5. The number of embryos/animals analyzed is showed in the columns. Genotype was analyzed by PCR. Significant differences are indicated by **, $p < 0.01$ and ***, $p < 0.001$.

3.2. Recording of $Ca_V1.2$ current in ventricular CMs

The whole-cell patch clamp technique was used to record current through L-type $Ca_V1.2$ channel, using barium as charge carrier in embryonic ventricular CMs. The embryonic CMs were isolated at day E18.5 and incubated at 37°C and 10% CO_2 for 24 h before electrophysiological recording. The measurements were performed with experimenter being unaware of the genotype, since the genotype of the embryos was determined after the recordings by PCR. Cell capacitances were not different in WT/WT, WT/Stop and Stop/Stop cardiomyocytes from ventricle, supporting the notion that the cell sizes of all these three genotype cardiomyocytes were similar (Fig. 8A).

Original recordings exhibited robust I_{Ba} in ventricular CMs from WT and WT/Stop embryos, whereas a tiny I_{Ba} was recorded in ventricular CMs from Stop/Stop embryos (Fig. 8B). Analysis of the current-voltage relationship displayed that the maximum of I_{Ba} was obtained at about 0 mV in CMs from all genotypes but that I_{Ba} was signifcantly reduced in ventricular CMs from Stop/Stop mice at all voltages examined. The current densities of WT/WT, WT/Stop and Stop/Stop at 0 mV were 69.43 ± 7.07 pA/pF, 59.29 ± 6.30 pA/pF and 6.70 ± 1.65 pA/pF, respectively. These results indicate that the postpartum death of the Stop/Stop mice is caused possibly by a massive reduction of the L-type calcium current in isolated ventricular CMs.

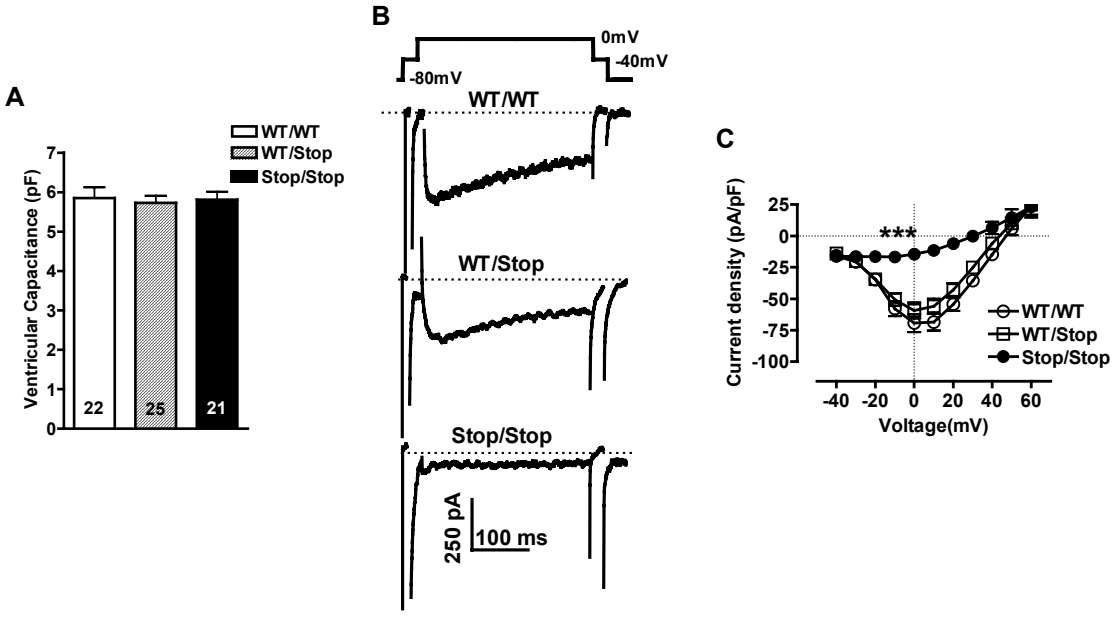

Fig. 8 Electrophysiological analysis of isolated ventricular CMs from E18.5 hearts. A, cell capacitances of ventricular CMs from WT/WT (*open columns*), WT/Stop (*hatched columns*) and Stop/Stop (*black columns*) mice. Columns represent means ± SEM. Numbers indicate the number of CMs. Data sets were not statistically different which were evaluated by ANOVA followed by Bonferroni post-test. B, original recordings of I_{Ba}. CMs were stimulated by the voltage pulse depicted above. C, current-voltage relationship of I_{Ba}. Cardiac cells were isolated from at least three embryos obtained from three independent pregnant mothers. Current is expressed as current density. Data points represent means ± SEM with n = 12-17. Asterisks indicate a statistically significant difference (***, $p < 0.001$) between the data sets from Stop/Stop and WT mice. Statistical analysis was performed by 2-way ANOVA followed by Bonferroni post-test. Genotype was analyzed by PCR.

3.3. Western blot analysis of $Ca_V1.2$

The Western blot analysis of $Ca_V1.2$ was performed by Dr. Katrin Domes. The expression of $Ca_V1.2$ was checked in heart and smooth muscle tissues from Stop/Stop mice by Western blot analysis. The signal for $Ca_V1.2$ was reduced in hearts from Stop/Stop mice compared with the hearts from WT mice (Fig. 9). However, the signal for $Ca_V1.2$ was identical in the smooth muscle tissues from Stop/Stop mice and WT mice. These findings indicate that the truncated $Ca_V1.2$ channel is differentially processed in heart and smooth muscle. Interestingly, it was proposed that heart and smooth muscle

express different isoforms of the $Ca_V1.2$ channel, termed $Ca_V1.2a$ and $Ca_V1.2b$, or alternatively named HK1 and LK1 (Biel *et al.*, 1990; Hu *et al.*, 1998; Hullin *et al.*, 1992; Welling *et al.*, 1997), which differ only by 5% and are expressed in distinct cells. The "cardiac ($Ca_V1.2a$)" channel is predominantly expressed in CMs, whereas the "smooth muscle ($Ca_V1.2b$)" channel is mainly expressed in the smooth muscle but not in the CMs (Cheng *et al.*, 2007; Welling *et al.*, 1997). Actually, $Ca_V1.2a$ and $Ca_V1.2b$ are alternatively spliced from the same $Ca_V1.2$ channel gene; therefore, the truncation of the $Ca_V1.2$ channel gene at Asp-1904 should cause two truncated isoforms. These findings indicate that the truncated $Ca_V1.2$ channel may be functional in smooth muscle but not in cardiac muscle.

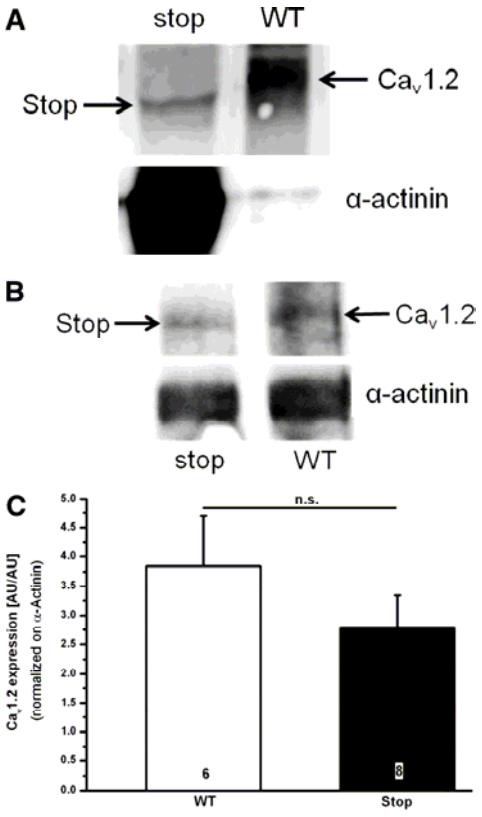

Fig. 9 $Ca_V1.2$ expression in heart and non-heart tissues. A, Western blot of cardiac tissue from WT and Stop/Stop E18.5 embryos. Upper panel, $Ca_V1.2$; lower panel, α-actinin as loading control. Please note that quite different amounts of protein were loaded: 2 (WT) and 50 (Stop) µg proteins extract per slot. B, Western blot of non-cardiac, non-brain tissue from WT and Stop/Stop E18.5 embryos. Upper panel, $Ca_V1.2$; lower panel, α-actinin as loading control. 150 µg protein extract were loaded per slot. C, statistics of the

density of $Ca_V1.2$ band shown as arbitrary units normalized for the α-actinin loading control. Tissues were obtained from embryos of six to eight mothers. Samples were electrophoresed on a 6% SDS-PAGE. n.s., not significantly different. AU, arbitrary units.

3.4. Expression of truncated $Ca_V1.2$ channel in HEK293 cells

Previous Western blot analysis supported the conclusion that distinct expression of the truncated isoforms of the $Ca_V1.2$ channel in cardiac ($Ca_V1.2a$) and smooth ($Ca_V1.2b$) muscle cells. Further, we tested this concept by transfecting HEK293 cells with the truncated form of Cav1.2a (HK1) and Cav1.2b (LK1).

3.4.1. Recording of $Ca_V1.2$ current in HEK293 cells transfected with HK1 and $HK1^{Stop}$ constructs

The HK1 ($Ca_V1.2a$) sequences were truncated at Ser-1905 in the rabbit cDNA, which corresponds to Asp-1904 in the murine $Ca_V1.2$ gene, yielding $HK1^{Stop}$ channel. HEK293 cells were transfected with the rabbit $Ca_V1.2$ channel isoform HK1, which is predominantly expressed in rat and mouse heart (Link *et al.*, 2009; Welling *et al.*, 1997), or its mutation $HK1^{Stop}$, together with the $Ca_V\beta_{2a}$ and $Ca_V\alpha_2\delta$ subunits. The transfected cells were seeded on poly-(L)-lysine-coated plates for electrophysiological studies.
Original recordings in Fig. 10A show the I_{Ba} in HEK293 cells transfected with $HK1^{Stop}$ channel was obviously decreased. HEK293 cells transfected with $HK1^{Stop}$ channel almost had no I_{Ba} compared with cells transfected with the full-legth HK1 construct. Analysis of the current-voltage relationship showed that the maximum of I_{Ba} was obtained at about +20 mV in transfected HEK293 cells but that I_{Ba} was signifcantly reduced in $HK1^{Stop}$ at all voltages examined. The current densities of HK1 and $HK1^{Stop}$ at +20 mV were -90.35 ± 10.61 pA/pF and -12.14 ± 2.28 pA/pF, respectively. These findings indicate that the truncated $HK1^{Stop}$ corresponding to truncated $Ca_V1.2a$ in heart also has low I_{Ba} *in vitro*.

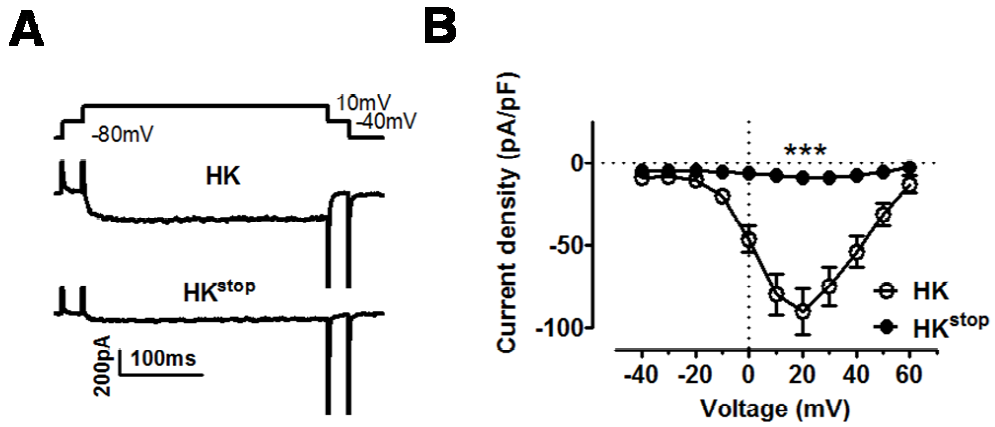

Fig. 10 Electrophysiological recordings of HK1 and HK1^{Stop} in transfected HEK293 cells. A, original recordings of I_{Ba}. HEK293 were transfected with HK1 or HK1^{Stop} channel. Cells were stimulated by the voltage pulse depicted above. B, current-voltage relationship of I_{Ba}. HEK293 cells were transfected with HK1 and HK1^{Stop}. Current is expressed as current density. Data points represent means ± SEM with HK1 n = 20 and HK1^{Stop} n = 12. Asterisks indicate a statistically significant difference (***, $p < 0.001$)

3.4.2. Recording of $Ca_V1.2$ current in HEK293 cells transfected with LK1 and LK1^{Stop} constructs

The LK1 ($Ca_V1.2b$) sequence was truncated at Ser-1905, corresponding to Asp-1904 in the murine $Ca_V1.2$ gene, yielding a LK1^{Stop} sequence. HEK293 cells were transfected with the rabbit $Ca_V1.2$ channel isoform LK1, which is predominantly expressed in the smooth muscle (Link *et al.*, 2009; Welling *et al.*, 1997), or its mutation LK1^{Stop}, together with the $Ca_V\beta_{2a}$ and $Ca_V\alpha_2\delta$ subunits. Electrophysiological analysis revealed that HEK293 cells transfected with LK1 and its mutation LK1^{Stop} exhibited robust I_{Ba} (Fig. 11B and C). The current densities of LK1 and LK1^{Stop} at +20 mV were -113.44 ± 17.81 pA/pF and -90.53 ± 29.32 pA/pF, respectively. These results confirm the Western blot analysis of Stop embryos that there is a distinct expression of the truncated isoforms of the $Ca_V1.2$ channel in cardiac and smooth muscle cells.

3.4.3. Recording of $Ca_V1.2$ current in HEK293 cells transfected with LK4^{Stop} construct

The amino acid sequence LK1 ($Ca_V1.2b$) and HK1 ($Ca_V1.2a$) differ only at four sites (A, B, C, D, see Fig. 11A), namely, the amino terminus, the IS6 and IVS3 transmembrane segments as well as an insert in the cytoplasmic loop connecting domain I and domain II which is only present in the LK1 subunit. To identify whether or not these sites are responsible for the different properties of the $LK1^{Stop}$ and $HK1^{Stop}$, we created an LK splice variant that differs only at the A part of the amino acid sequence (LK4). The LK4 sequence was truncated at Ser-1905, corresponding to Asp-1904 in the murine $Ca_V1.2$ sequence yielding a $LK4^{Stop}$ channel for comparison. Electrophysiological analysis revealed that HEK293 cells transfected with $LK4^{Stop}$ exhibited robust Ca^{2+} currents which were identical with full-length LK1 (Fig. 11B and C). These findings indicate that the different amino terminus of LK1 and HK1 determine the distinct expression of the truncated $Ca_V1.2$ channel in the respective tissue.

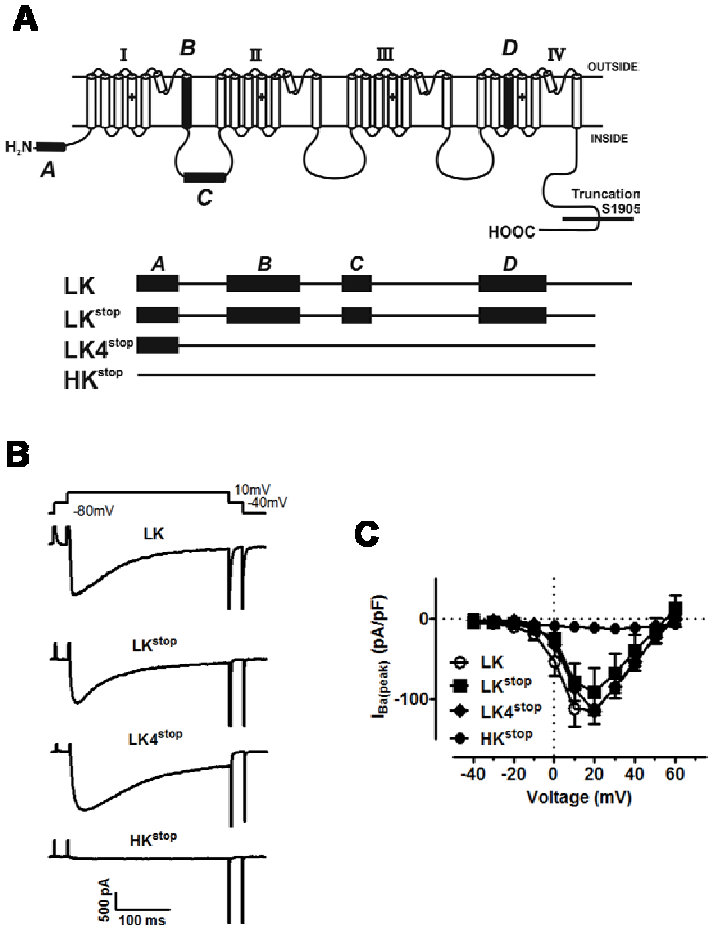

Fig. 11 Scheme for splice variants of HK1 ($Ca_V1.2a$) and LK1 ($Ca_V1.2b$) sequence. All transfections were concomitantly performed with $Ca_V\beta_{2a}$ and $Ca_V\alpha_2\delta$ cDNA. A, scheme for splice variants of $Ca_V1.2$. The

black boxes labeled A, B, C, and D indicate the differences between the HK1 ($Ca_V1.2a$) and smooth muscle LK1 ($Ca_V1.2b$). The $HK1^{Stop}$ and $LK1^{Stop}$ were truncated at Ser-1905, which correspond to Asp-1904 in the murine $Ca_V1.2$ sequence. $LK4^{Stop}$ contains the sequence of the cardiac $HK1^{Stop}$ ($Ca_V1.2a$) with the exception that the amino terminus is the smooth muscle exon 1b (box A). B, original recordings of I_{Ba}. HEK293 cells were transfected with LK1, $LK1^{Stop}$, $LK4^{Stop}$ and $HK1^{Stop}$. C, current-voltage relationship of I_{Ba}. HEK293 cells were transfected with LK1, $LK1^{Stop}$, $LK4^{Stop}$ and $HK1^{Stop}$. Current is expressed as current density. Curves for LK1, $LK1^{Stop}$, and $LK4^{Stop}$ were not statistically different. Data points represent means ± SEM with n = 7 for LK1, n = 13 for $LK1^{Stop}$, n = 6 for $LK4^{Stop}$ and n = 12 for $HK1^{Stop}$.

3.4.4. Western blot analysis of HEK293 cells transfected with LK1, HK1, $LK1^{Stop}$, $HK4^{Stop}$ and $LK4^{Stop}$

The Western blot analysis of HEK293 cells transfected with LK1, HK1, $LK1^{Stop}$, $HK4^{Stop}$ and $LK4^{Stop}$ was performed by Dr. Katrin Domes. Proteins were seperated on an 8% or a 6% SDS-PAGE gel, using GAPDH as loading control. The Western blot analysis confirmed the results we obtained by the electrophysiological measurement. Western blot analysis confirmed that a minor expression of the $HK1^{Stop}$ channel in HEK293 cells, in contrast to a robust expression of the $Ca_V1.2$ channel in HEK293 cells transfected with the LK1, HK1, $LK1^{Stop}$ and $LK4^{Stop}$ channel.

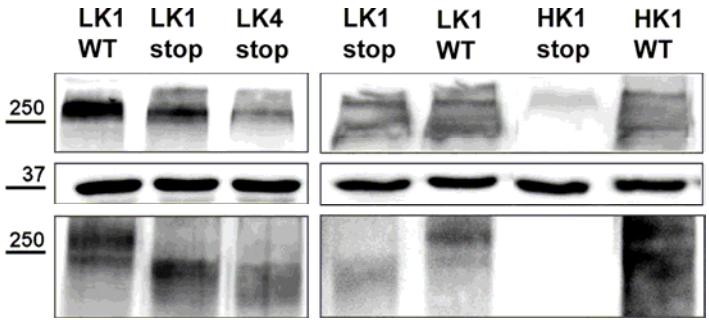

Fig. 12 Western blot of HEK293 cells transfected with HK1, LK1 and the corresponding truncated constructs. Proteins were separated on an 8% (upper and middle panel) or a 6% (bottom panel) SDS-PAGE gel. The middle panel shows GAPDH as a loading control, the upper and bottom panels show $Ca_V1.2$ protein. 20 µg proteins were loaded per slot. The left three lanes and the right four lanes were from distinct gels. Transfection and Western blotting were repeated five times.

3.4.5. Effect of proteasome inhibitors in transfected HEK293 cells

HEK293 cells transfected with the $HK1^{Stop}$ showed reduced I_{Ba} and $Ca_V1.2$ protein expression. These results may represent a defect in transcription, translation or protein processing which targets the $Ca_V1.2$ channel to the membrane. Recently, it has been suggested that $Ca_V1.2$ channel allows ubiquitination followed by proteasomal degradation of the translated protein (Altier *et al.*, 2011; Rougier *et al.*, 2011; Waithe *et al.*, 2011). Therefore, we tested whether or not inhibition of intracellular proteolysis affected the expression of the $Ca_V1.2$ channel.

3.4.5.1. Effect of proteasome inhibitors in HEK293 cells transfected with $HK1^{Stop}$

For this purpose, the proteasome inhibitors lactacystin (10 μM) and MG132 (10 μM) were used. It has been reported that lactacystin and MG132 induced apoptotic cell death at high dose or long incubation time (Zhou *et al.*, 2010). Therefore, we treated transfected HEK293 cells in presence of lactacystin+MG132 (10 μM) for 4 h, 8 h and 12 h. As Fig. 13 shows, lactacystin+MG132 time-dependently increased the I_{Ba} in HEK293 cells transfected with $HK1^{Stop}$ construct. We finally chose 12 h as incubation time of proteasome inhibitor in order to maximize the current amplitude.

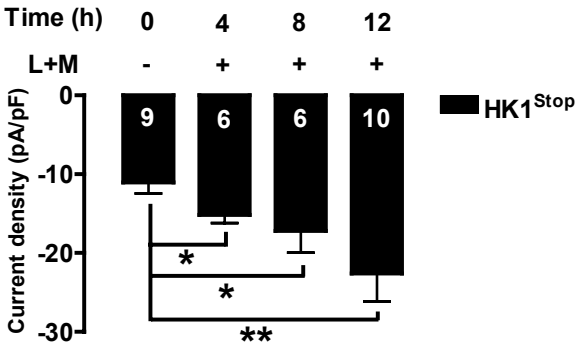

Fig. 13 Time-depedent increased I_{Ba} in transfected HEK293 cells with $HK1^{Stop}$ construct. Columns points represent means ± SEM. The number of cells analyzed is showed in the columns. Significant differences are indicated by *, $p < 0.05$ and **, $p < 0.01$.

Following, cells were treated with proteasome inhibitors for the last 12 h. Extracellular perfusion of lactacystin together with MG132 obviuosly increased the current amplitude in HK1^{Stop} transfected HEK293 cells. After treatment with lactacystin together with MG132 the current density of HK1^{Stop} increased by almost 2-fold to -25.38 ± 2.02 pA/pF from -12.14 ± 2.28 pA/pF (Fig. 14). However, the I_{Ba} of HK1^{Stop} transfected cells incubated with lactacystin+MG132 (10 µM) for 12 h was still lower than the I_{Ba} recorded in HEK293 cells transfected with full-length HK1. There was no significant difference of the I_{Ba} recorded in HEK293 cells transfected with full-length HK1 before and after incubation with lactacystin together with MG132.

Bortezomib is a new proteasom inhibitor that is used in humans and seems to be less toxic to cells. No or less apototic effects have been reported in cell cultures (Adams *et al.*, 2004). Therefore, we incubated HEK293 cells transfected with HK1^{Stop} with bortezomib (10 µM) for 12 h. Treatment with bortezomib increased 2-fold of I_{Ba} in HEK293 cells transfected with HK1^{Stop}. The by bortezomib enhanced I_{Ba} can be blocked by 1 µM isradipine (ISR). These results indicate that the truncated HK1^{Stop} channel is degraded in the proteasome after translation in HEK293 cells.

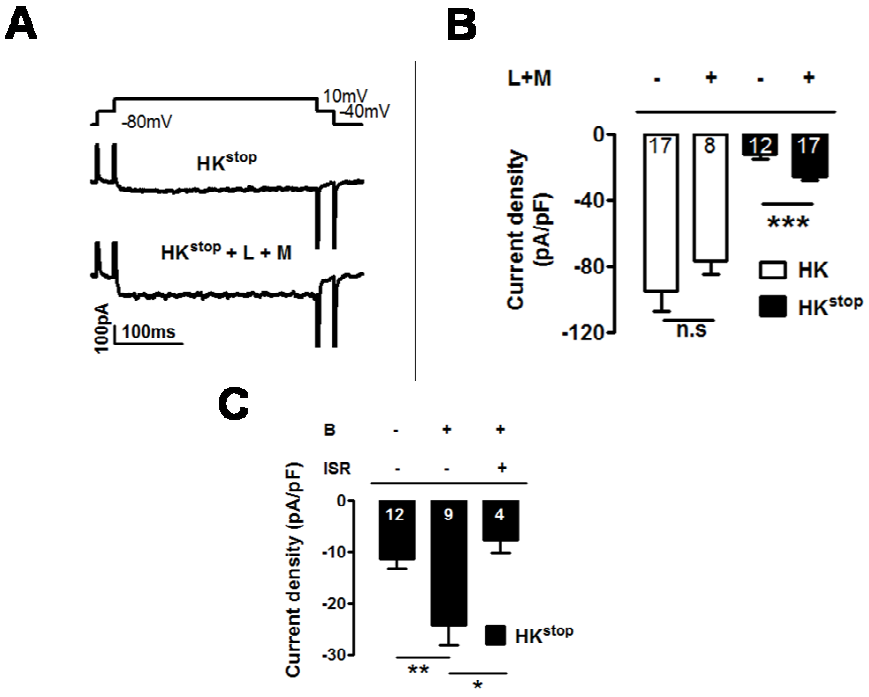

Fig. 14 Treatment of HK1^{Stop} with proteasome inhibitors. A, original recordings of I_{Ba} in HEK293 cells transfected with the truncated HK1^{Stop} construct. Cells were treated with lactacystin (10 µM) and MG132

(10μM) for the last 12 h. Cells were stimulated by the voltage pulse depicted above. B, current density of I_{Ba} elicited at 20 mV. HEK293 cells transfected with full-length HK1 and the truncated $HK1^{Stop}$. Transfected cells were incubated in the absence or presence of lactacystin+MG132 (10 μM each) for the last 12 h. C, maximal current density of I_{Ba} in HEK293 cells transfected with the truncated $HK1^{Stop}$. Transfected cells were incubated in the absence or presence of bortezomib (10 μM) for the last 12 h. I_{Ba} recordings were determined also in the presence of isradipine (ISR, 1 μM) in some cells treated with bortezomib. Columns represent means ± SEM. The number of cells analyzed is showed in the columns. Asterisks indicate a statistically significant difference by *, $p < 0.05$, **, $p < 0.01$ and ***, $p < 0.001$; n.s., non-significant.

Western blot analysis was performed by Dr. Katrin Domes. HEK293 cells were transfected with the full-length HK1 or the truncated $HK1^{Stop}$ construct together with $Ca_V\beta_{2a}$ and $Ca_V\alpha_2\delta$ cDNA and treated for 48 h, then incubated in the absence or presence of lactacystin+MG132 (10 μM) or bortezomib (10 μM) for 12 h. Treatment of lactacystin+MG132 (10 μM) (Fig.15A) or bortezomib (10 μM) (Fig.15B) for 12 h significantly up-regulated the expression of the $HK1^{Stop}$, but had no effect in HEK293 cells transfected with full-length HK1 confirming the electrophysiological data.

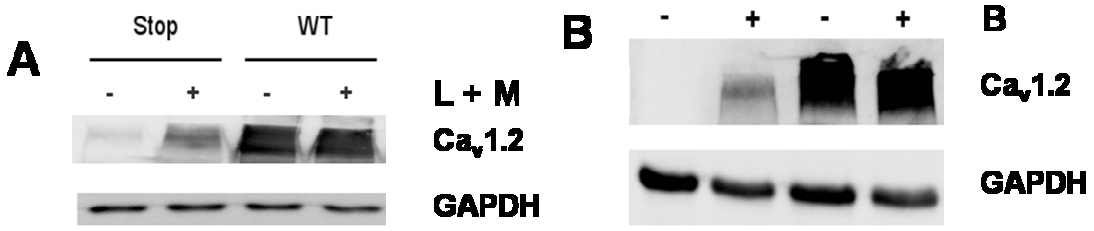

Fig. 15 Western blot analysis of proteasome inhibitors for $HK1^{Stop}$. A and B, Western blot from HEK293 cells transfected with the full-length HK1 or the truncated $HK1^{Stop}$ construct together with $Ca_V\beta_{2a}$ and $Ca_V\alpha_2\delta$ cDNA in the absence and presence of lactacystin (L; 10 μM) and MG132 (M; 10 μM). A, in the absence and presence of bortezomib (B; 10 μM). B, cells were cultured for 48 h before proteasome inhibitors were added for the last 12 h. Proteins were separated on an 8% SDS-PAGE gel. Transfection and Western blots were repeated at least three times with similar results.

3.4.5.2. Effect of bortezomib in HEK293 cells transfected with $LK1^{Stop}$

Further, we tested whether inhibition of intracellular proteolysis affected the expression of the $LK1^{Stop}$ channel. HEK293 cells were transfected with the LK1 and $LK1^{Stop}$ constructs. As we can see in Fig. 12, the current densities of $LK1^{Stop}$ were -90.53 ± 29.32 pA/pF and -81.55 ± 11.32 pA/pF, respectively, with and without bortezomib (10 μM). The bortezomib had no effect on I_{Ba} of cells transfected with the $LK1^{Stop}$ construct.

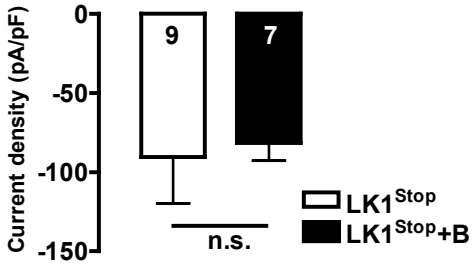

Fig. 16 Current density of I_{Ba} in absence or presence of bortezomib in HEK293 cells transfected with the truncated $LK1^{Stop}$. Cells were or were not treated with bortezomib (10μM) for the last 12 h. Columns represent means ± SEM with n = 9 for LK^{Stop} and n = 7 for LK^{Stop} + B. n.s., not significantly different.

3.5. Effect of bortezomib on I_{Ba} in ventricular CMs from Stop/Stop mice

Next, we tried to figure out if the same mechanism operated in the embryonic ventricular CMs. The embryonic ventricular cardiomyocytes were isolated from hearts of WT, WT/Stop and Stop/Stop mice at E18.5 embryos and cultured in the absence or presence of bortezomib (10 μM) to further investigate whether the reduced $Ca_V1.2$ current can be rescued or not. In the presence of 10 μM bortezomib, the current density of Stop/Stop CMs was doubled. However, no effect was observed in the WT/WT and WT/Stop CMs with 10 μM bortezomib (Fig. 17). These results indicate that inhibition of the proteasomal pathway rescues partially I_{Ba} in CMs expressing the truncated $Ca_V1.2$ channel. Obviously, the truncated $Ca_V1.2$ Stop channels are degraded in the proteasome after translation in murine CMs.

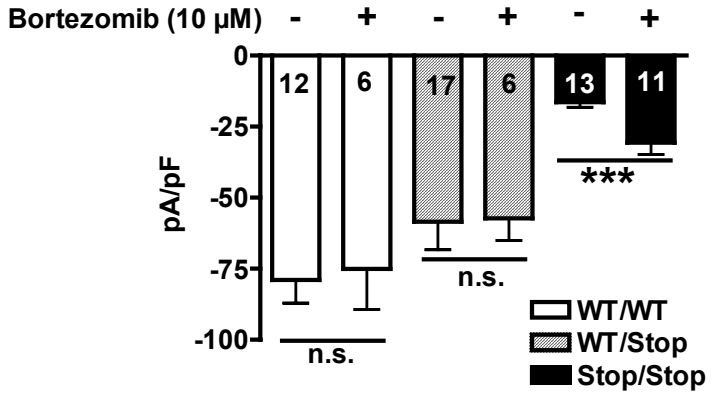

Fig.17 Rescue of the truncated Stop $Ca_V1.2$ channel by bortezomib. Current density of I_{Ba} in ventricular CMs from WT/WT (*open columns*), WT/Stop (*hatched columns*), and Stop/Stop (*black columns*) mice. CMs were or were not treated with bortezomib (10 µM) for the last 12 h. Columns represent means ± SEM with n = 6 - 17 from four to six embryos. Statistical analysis was performed by 2-way ANOVA followed by Bonferroni post-test. Significant differences are indicated by ***, $p < 0.001$; *n.s.*, non-significant. Genotype was analyzed by PCR.

3.6. Effect of isoproterenol on I_{Ba} in ventricular CMs

As reported, C-terminus of $Ca_V1.2$ serves as the substrate for β-adrenergic activation of CMs, which can increase the maximal probability of channel opening and Ca^{2+} current amplitude (Bunemann *et al.*, 1999; Catterall, 2000b; Hulme *et al.*, 2004). To investigate β-adrenergic regulation, we superfused CMs with 100 nM isoproterenol (Iso), a direct activator of β-adrenergic receptors. The pulse protocols as well as original current waveforms are showed in Fig. 18A and corresponding statistcal analysis is displayed in Fig. 18B. From the original recording and analytical graph we can see that isoproterenol (100 nM) increased I_{Ba} in ventricular CMs from WT and WT/Stop mice by about 50% (Fig. 18), whereas I_{Ba} was not affected by isoproterenol in ventricular CMs from Stop/Stop mice.

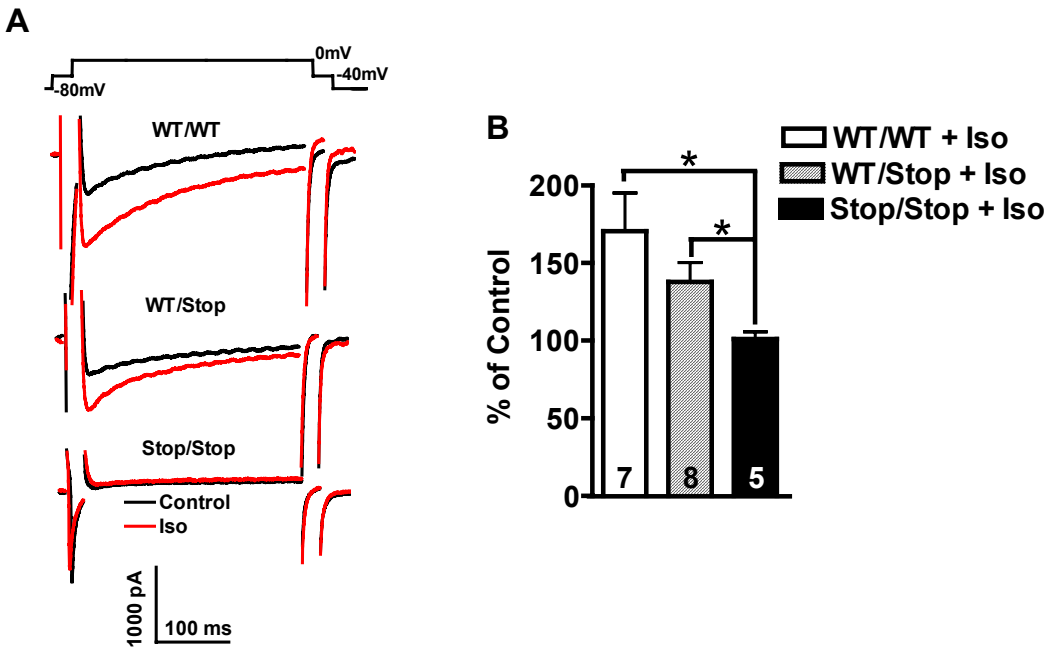

Fig. 18 Effect of isoproterenol on I_{Ba} in ventricular CMs from murine embryos (E18.5). A, original recordings of I_{Ba} in ventricular CMs from WT, WT/Stop and Stop/Stop mice. Currents were recorded in the absence (control) and presence of 100 nM Iso. B, statistics of Iso-dependent increase in peak current of ventricular CMs from WT/WT (*open columns*), WT/Stop (*hatched columns*), and Stop/Stop (*black columns*) mice. Columns represent means ± SEM normalized to basal current values. Number of recorded cells is given in columns. Statistical analysis was performed by Student t-test. Asterisks indicate a statistically significant difference (*, $p < 0.05$).

3.7. Effect of forskolin on I_{Ba} in ventricular CMs

A robust coupling of β-adrenergic receptors to G proteins is not fully extablished until birth (An *et al.*, 1996). Therefore, adenylyl cyclase, downstream of β-adrenergic receptors and G proteins, was activated directly using forskolin (FSK) to study the regulation of I_{Ba} by the β-adrenergic signaling cascade. Similar to Iso, FSK (5 µM) increased by 80% the current density of I_{Ba} in ventricular CMs from WT and WT/Stop mice, but had no effect in ventricular CMs from Stop/Stop mice (Fig. 19). These findings indicate that the $Ca_V1.2$ truncated at Asp-1904 was not affected significantly the β-adrenergic signaling cascade in ventricular CMs most likely because only minimal amounts of the truncated channel were incorporated into the membrane.

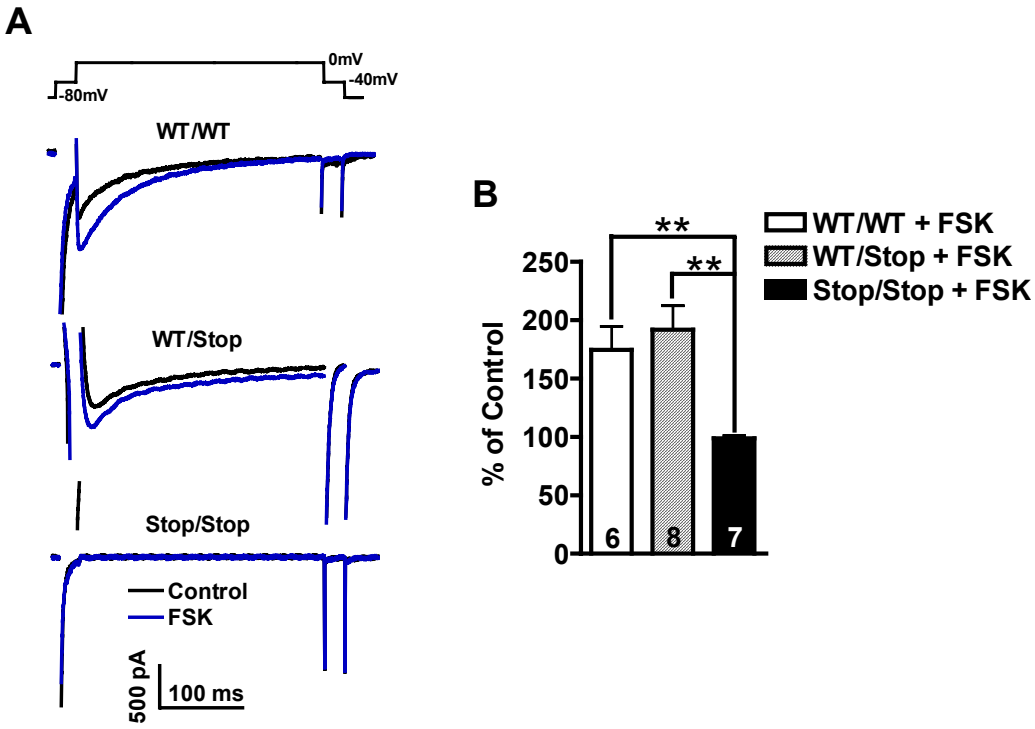

Fig. 19 Effect of forskolin on I_{Ba} in ventricular CMs from murine embryos (E18.5). A, original recordings of I_{Ba} in ventricular CMs from WT, WT/Stop and Stop/Stop mice. Currents were recorded in the absence (control) and presence of 5 µM FSK. B, statistics of forskolin-dependent increase in peak current of ventricular CMs from WT/WT (*open columns*), WT/Stop (*hatched columns*), and Stop/Stop (*black columns*) mice. Columns represent means ± SEM normalized to basal current values. Number of recorded cells is given in columns. Statistical analysis was performed by Student t-test. Asterisks indicate a statistically significant difference (**, $p < 0.01$).

3.8. Recording of $Ca_V1.2$ current in atrial CMs

The previous results showed that the truncated $Ca_V1.2$ channel was differentially processed in ventricular CMs and smooth muscle tissues. It has been reported that atrial CMs display different pattern of Ca_V channels, as well as different physiological and anatomical properties compared with ventricular CMs (Fu *et al.*, 2011), regarding the rudimentary transverse-axial tubular network, the expression levels of key proteins involved in Ca^{2+} signaling and homeostasis (Bootman *et al.*, 2011). Therefore, the possibility existed that atrial CMs may also exhibit a differential processing of the

truncated Cav1.2 channel. Consequently, we comparatively analyzed I_{Ba} in atrial CMs at E18.5 from WT, WT/Stop and Stop/Stop mice.

Cell capacitances were not different in WT/WT, WT/Stop and Stop/Stop CMs from atria supporting the notion that the cell sizes of all these atrial CMs expressing different genotypes were similar (Fig.20 A). We can see from the original recording and I-V relationship and in contrast to ventricular CMs from Stop/Stop mice (-12.14 ± 2.28 pA/pF), a robust I_{Ba} was recorded in atrial CMs from Stop/Stop mice (-44.81 ± 7.40 pA/pF) (Fig. 20B and C). The current densities recorded in atrial CMs from WT and WT/Stop mice at 0 mV were -74.50 ± 17.42 pA/pF and -70.09 ± 12.98 pA/pF, respectively, showing no difference (Fig. 20B and C). All these measurements were performed in blind mode. The genotype of the pups was determined by PCR after the recordings.

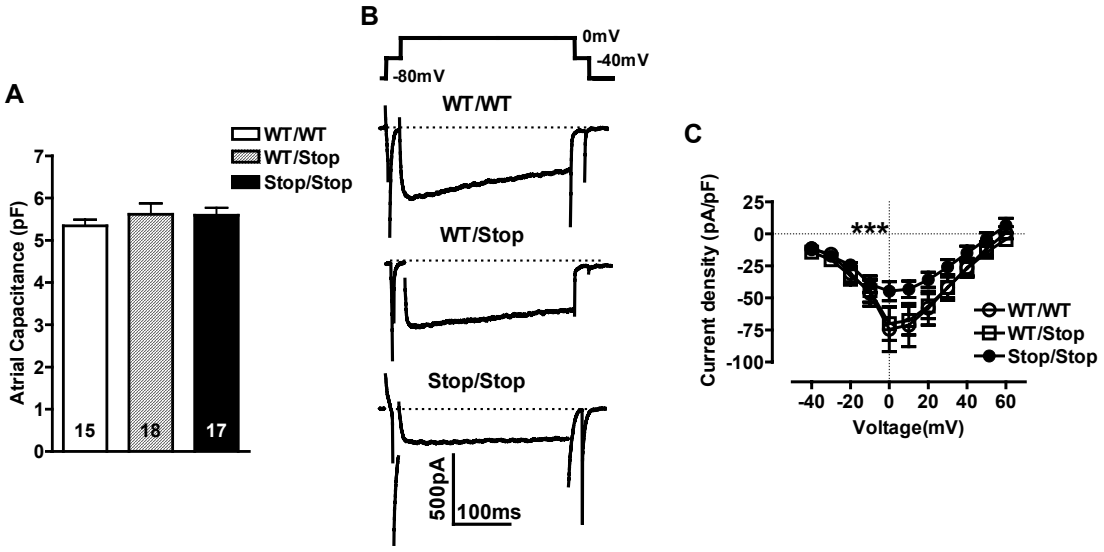

Fig. 20 I_{Ba} recordings in atrial CMs from murine embryos (E18.5). A, cell capacitances of atrial CMs from WT/WT (*open columns*), WT/Stop (*hatched columns*) and Stop/Stop (*black columns*) mice. Columns represent means ± SEM. Numbers indicate the number of CMs. Data sets were not statistically different as indicated by ANOVA followed by Bonferronipost-test. B, original recordings of I_{Ba} in atrial CMs from WT, WT/Stop, and Stop/Stop mice. C, current-voltage relationship of I_{Ba} recorded in atrial CMs from WT, WT/Stop and Stop/Stop mice. Data points represent means ± SEM with n = 9-22. Asterisks indicate a

statistically significant difference (***, $p < 0.001$) between the data sets from Stop/Stop and WT mice. Statistical analysis was performed by 2-way ANOVA followed by Bonferroni post-test.

3.9. Effect of forskolin on I_{Ba} in atrial CMs

It has been reported that atrial CMs exhibit robust L-type Ca^{2+} channel currents that can be enhanced by β-adrenergic stimulation (Ouadid *et al.*, 1991). As we had shown above, atrial CMs from Stop/Stop mice also exhibited a robust I_{Ba} compared with ventricular CMs from Stop/Stop mice. Therefore, we further investigated the effect of β-adrenergic stimulation in atrial CMs at E18.5.

Atrial CMs were stimulated with FSK to investigate whether or not the mutation at Asp-1904 had an effect on β-adrenergic signaling cascade regulation of I_{Ba} in atrial CMs from Stop/Stop mice. The pulse protocols as well as original current waveforms are shown in Fig. 21A and the corresponding statistcal anaysis is displayed in Fig. 21B. From the original recording and analytical graph we can see that foskolin (5 μM) increased I_{Ba} in atrial CMs from WT and WT/Stop mice by about 100% (Fig. 21A and B), surprisingly, I_{Ba} was also 2 fold up-regulated by FSK in atrial CMs from Stop/Stop mice (Fig. 21A and B). These findings indicate that the β-adrenergic signaling cascade in atrial CMs is not influenced by the Stop mutation in the $Ca_V1.2$ gene. The differential effect of FSK in ventricular and atrial CMs may indicate a different coupling of the respective L-type Ca^{2+} currents to the β-adrenergic signaling cascade in ventricle and atrium or point to the expression of different types of Ca_V channels mediating L-type Ca^{2+} currents in ventricle and atrium.

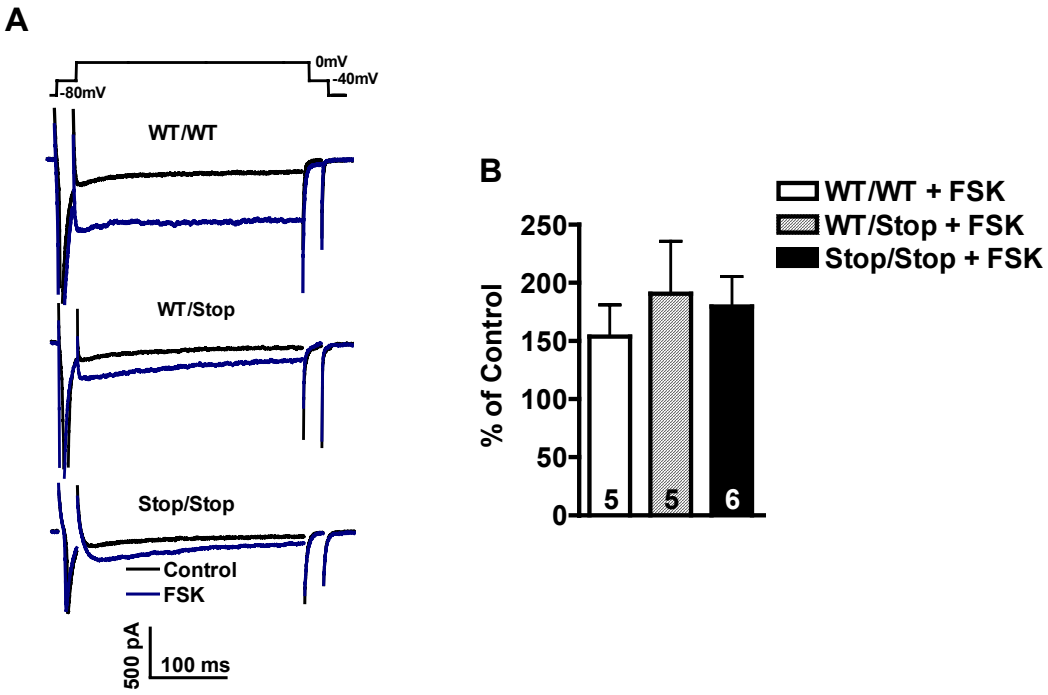

Fig. 21 Effect of forskolin on I_{Ba} in atrial CMs from murine embryos (E18.5). A, original recordings of I_{Ba} in atrial CMs from WT, WT/Stop and Stop/Stop mice. Currents were recorded in the absence (control) and presence of 5 µM forskolin (FSK). B, statistics of forskolin-dependent increase in peak current of atrial CMs from WT/WT (*open columns*), WT/Stop (*hatched columns*) and Stop/Stop (*black columns*) mice. Columns represent means ± SEM normalized to basal current values. Number of recored cells is given in columns. Statistical analysis was performed by Student t-test revealing no statistically significant difference between the data.

3.10. Voltage-dependent activation curves of I_{Ba} in ventricular and atrial CMs

The voltage-dependent activation curve of I_{Ba} in ventricular and atrial CMs were analyzed. The activation curves were fitted according to the Boltzmann equation. As Fig. 22A shows similar activation curves in ventricular CMs from WT and Stop/Stop mice, with half-maximal activation popential -22 mV and -20 mV, respectively. In contrast, the activation curve in atrial CMs from Stop/Stop mice was markedly shifted to the left by about 7 mV as compared with the curve obtained in atrial CMs from WT mice (Fig. 22B), with half-maximal activation popential -17 mV and -24 mV, respectively. These findings indicate that the L-type Ca^{2+} current in atrial CMs from Stop/Stop mice is possiblly carried by other Ca^{2+} channels, maybe $Ca_V1.3$ channels, since $Ca_V1.3$ channels

have been reported to display a more negative voltage-dependent activation curve as compared with $Ca_V1.2$ channels (Klugbauer *et al.*, 2002; Zhang *et al.*, 2005; Zhang *et al.*, 2002)

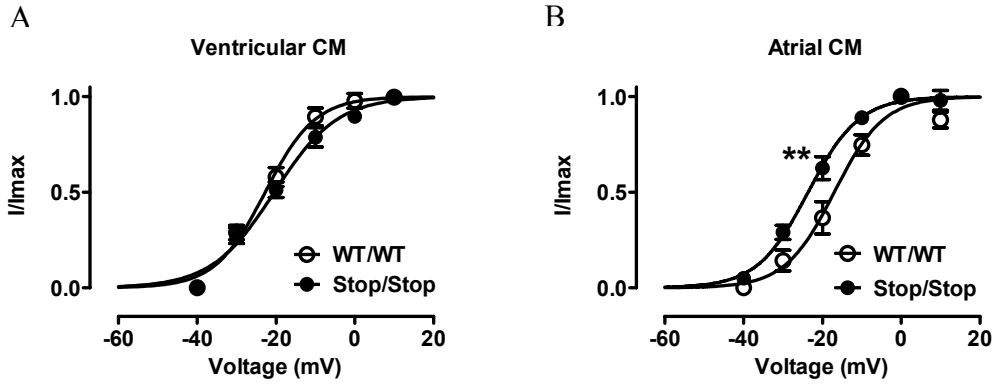

Fig. 22 Voltage-dependent activation curves of I_{Ba} in ventricular (A) and atrial (B) CMs from WT and Stop/Stop mice. Data points represent means ± SEM with n = 9 - 22. Curves represent a fit of the data sets with the Boltzmann equation ($r^2 > 0.97$). Voltages for half-maximal activation were -22 mV and -20 mV in ventricular CMs from WT and Stop/Stop mice (A), and -17 mV and -24 mV in atrial CMs from WT and Stop/Stop mice (B). Asterisks indicate a statistically significant difference (**, $p < 0.01$) between the data sets from Stop/Stop and WT mice. Statistical analysis was performed by 2-way ANOVA followed by Bonferronipost-test.

3.11. Effect of isradipine on I_{Ba} in ventricular and atrial CMs

We further comparatively analyzed the effect of isradipine on I_{Ba} in ventricular and atrial CMs. The dihydropyridine isradipine is known as a potent blocker of L-type Ca^{2+} currents through $Ca_V1.2$ channels displaying an IC_{50} value of about 0.4 μM (Hamilton *et al.*, 1987). The original current waveforms of ventricular and atrial CMs are shown in Fig. 23A and B and corresponding statistcal anaysis is displayed in Fig. 23C and D. From the original recording and analytical graph we can see that isradipine can significantly inhibit the I_{Ba} both in ventricular CMs and atrial CMs. 1 μM isradipine blocked about 65% of I_{Ba} in ventricular and atrial CMs from WT and WT/Stop mice (Fig. 23). The effects of 1 or 10 μM isradipine could hardly been seen in ventricular CMs from Stop/Stop mice (Fig. 23C), due to the minimal Ca^{2+} currents left. The inhition rate of 1 or 10 μM isradipine was not different. In contrast, the effects of 1 or 10 μM isradipine were obvious in atrial CMs from Stop/Stop mice with an inhibition of about 30 and 50% of control, respectively

(Fig. 23D). the different values suggest a reduced sensitivity of the Stop/Stop L-type current compared to the current in atrial CMs from WT mice.

It has been reported that L-type Ca^{2+} currents through $Ca_V1.3$ channels display a reduced sensitivity to dihydropyridines than through $Ca_V1.2$ channels (Koschak *et al.*, 2001). Atrial CMs are able to express $Ca_V1.3$ channels although the expression level of $Ca_V1.2$ channels is about 100x higher, at least in healthy human atrium (Gaborit *et al.*, 2007). This result further confirms the possibility that the L-type current recorded in atrial CMs from Stop/Stop mice may be carried by $Ca_V1.3$ channels.

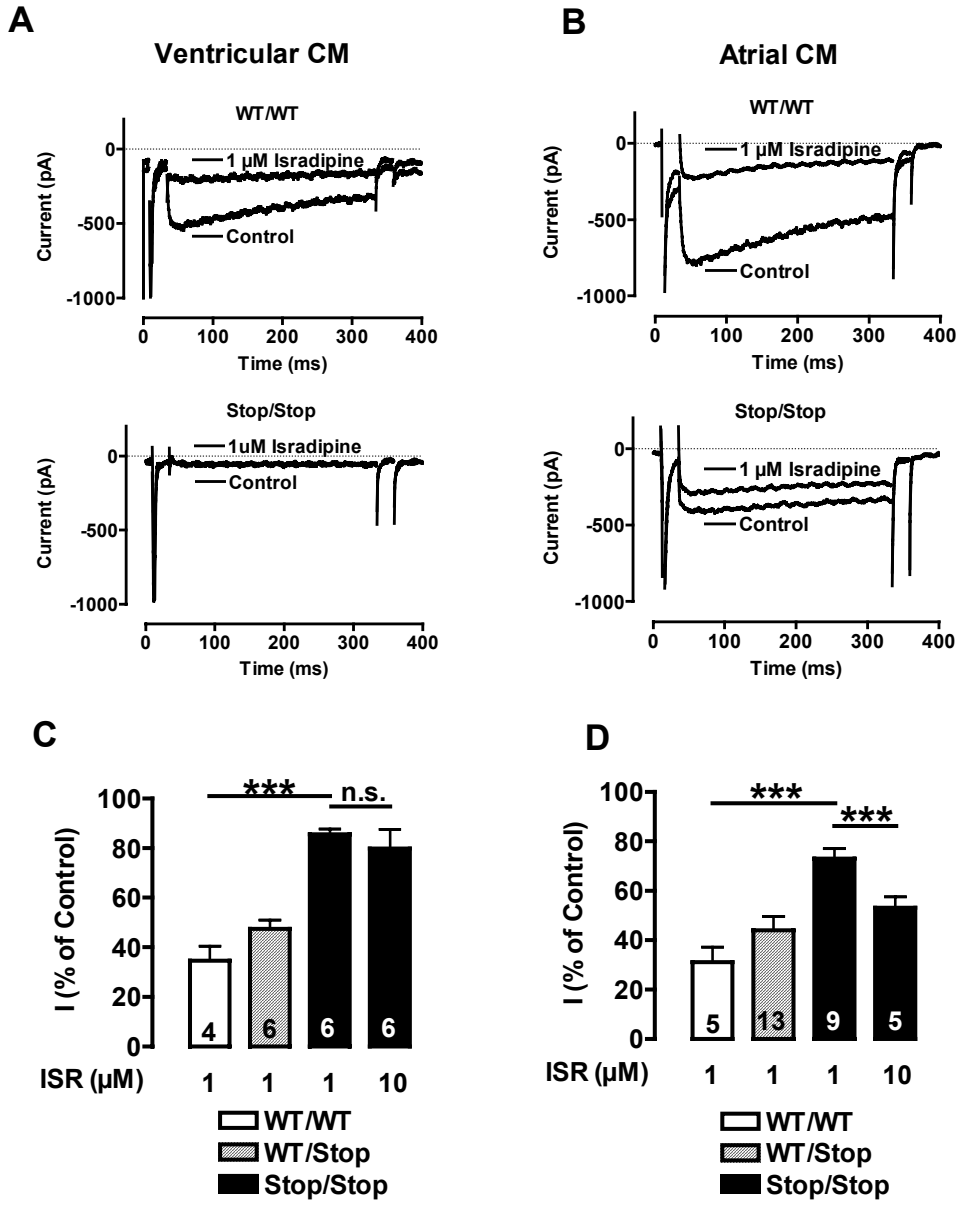

Fig. 23 Effect of isradipine on I_{Ba} in ventricular and atrial CMs from murine embryos. A and B, original recordings of I_{Ba} in ventricular (A) and atrial (B) CMs from WT and Stop/Stop mice. Currents were recorded with or without isradipine. C and D, effect of isradipine on the magnitude of I_{Ba} in ventricular (C) and atrial CMs (D). Columns represent means ± SEM normalized to basal current values. Number of recorded cells is given in columns. Numbers below the columns indicate the concentration of ISR used (1 or 10 μM). Statistical analysis was performed by Student t-test. Asterisks indicate a statistically significant difference (***, $p < 0.001$; n.s., non-significant).

3.12. Expression analysis of $Ca_V1.2$ in ventricular and atrial tissues from WT and Stop/Stop mice by RT-PCR

Consequently, we performed semi-quantitative reverse transcriptase polymerase chain reaction to evaluate the amount of mRNA for $Ca_V1.2a$, $Ca_V1.2b$, $Ca_V2.1$ and $Ca_V1.3$ channels in ventricular and atrial tissues at E18.5. The embryo genotype was determined by PCR. In order to compare expression levels obtained from independent experiments the data was normalized by using GAPDH or HPRT as internal standard. Fig. 24A, C, E and G show representative gels displaying the results from RT-PCR with total RNA isolated from ventricular or atrial tissues at E18.5. Signals for mRNA corresponding to the cardiac form of $Ca_V1.2$ ($Ca_V1.2a$), the smooth muscle form of $Ca_V1.2$ ($Ca_V1.2b$) and $Ca_V2.1$ were detected in ventricular and atrial tissues from WT and Stop/Stop mice and the signals were not statistically different. The expression levels of these three channels in both ventricular and atrial tissues were identical (Fig. 24A, B, C, D, G and H). Signals for mRNA corresponding to $Ca_V1.3$ in ventricular tissue from Stop/Stop mice were 2-fold reduced when compared with those from WT mice (Fig. 24E and F). In contrast, signals for mRNA corresponding to $Ca_V1.3$ were increased in atrial tissues from Stop/Stop mice when compared with those from WT mice (Fig. 24E and F). These findings are in aggreement with the above results indicating that atrial CMs from Stop/Stop mice increase the expression of $Ca_V1.3$ channels.

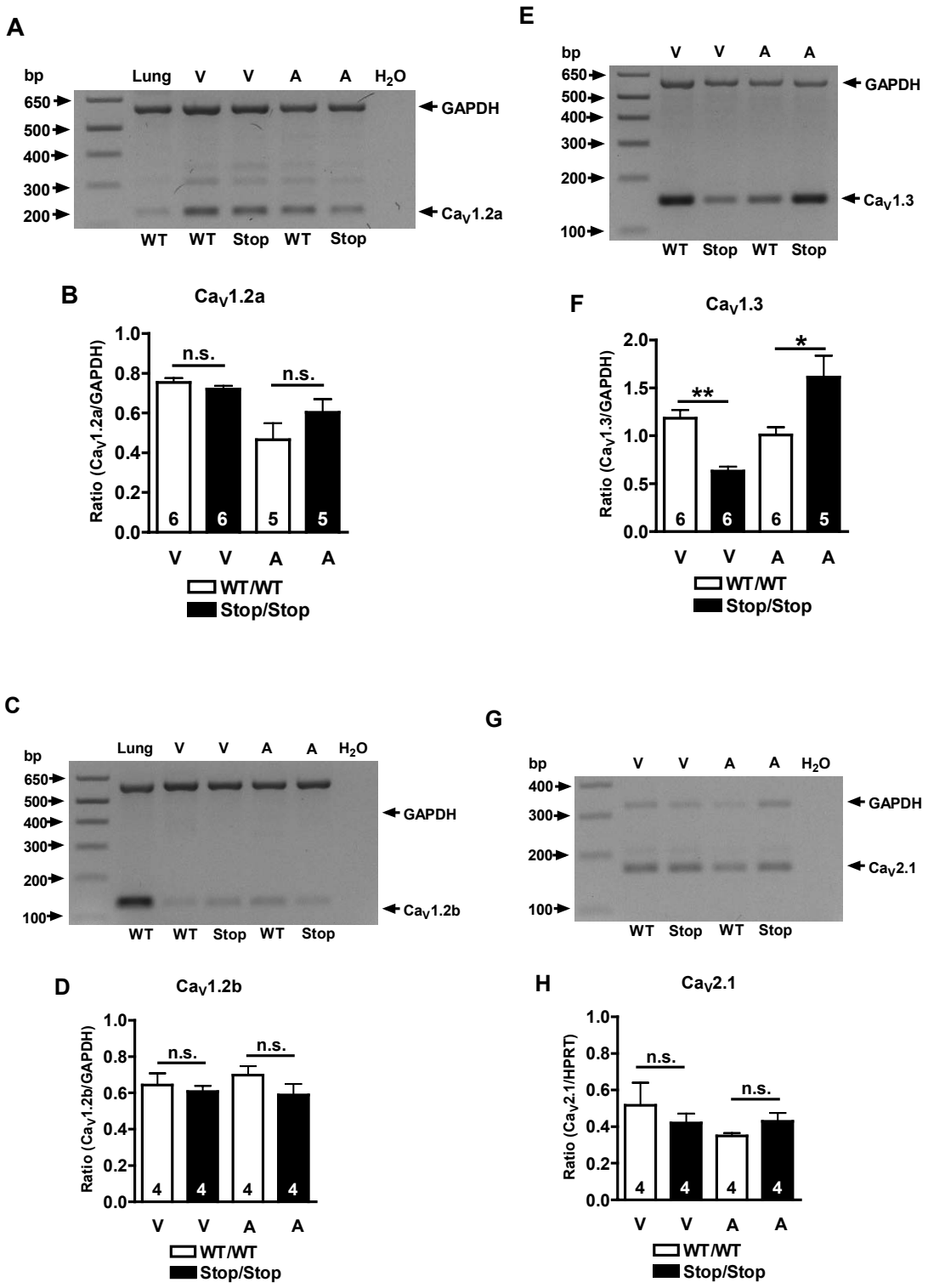

Fig. 24 Expression analysis of $Ca_V1.2$ channels in ventricular and atrial tissues from WT and Stop/Stop mice by RT-PCR. A, C, E and G, representative ethidium bromide-stained agarose gel of amplicons generated with primers against mRNA of $Ca_V1.2a$ (A), $Ca_V1.2b$ (C), $Ca_V1.3$ (E) and $Ca_V2.1$(G) in

ventricular (V) and atrial (A) tissues from WT and Stop/Stop mice. The size of the amplicons is indicated on the left (bp). Primers against mRNA for GAPDH or HPRT were used as control. In A, lung tissue from WT mice was used as a control for the specificity of the primers against mRNA of $Ca_V1.2a$. In C, lung tissue from WT mice was used as a control for the specificity of the primers against mRNA of $Ca_V1.2b$. B, D, F and H, quantitative analysis of the amplification products. Columns represent means ± SEM normalized to GAPDH (B, D, and F) or HPRT (H). Numbers in the columns indicate the number of experiments. Statistical analysis was performed by Student t-test. Asterisks indicate a statistically significant difference (*, $p < 0.05$; **, $p < 0.01$; n.s., non-significant).

4. Discussion

4.1. The role of truncated Cav1.2 at Asp-1904 in ventricular CMs

The C-terminus of $Ca_V1.2$, as carrier of a variety of potential regulatory structure elements, has been comprehensively investigated in cell culture expression studies and numerous results are obtained, which show how the C-terminus affects the function of the channel (Bunemann *et al.*, 1999; Davare *et al.*, 2001; Dolmetsch *et al.*, 2001; Dzhura *et al.*, 2000; Fuller *et al.*, 2010; Gao *et al.*, 2000; Gao *et al.*, 2001; Hulme *et al.*, 2006b). However, it is not certain which of the *ex vivo* observed effects are still present in the living mouse. Therefore, a mouse line expressing the truncated $Ca_V1.2$ channel was generated by introducing three stop codons after aspartate 1904 in the murine $Ca_V1.2$ gene corresponding to serine 1905 in the rabbit sequence. These three stop codons introduced after aspartate 1904 can stop the translation at this point, so that, ideally, the truncated protein was formed. The selection of the mutation site is based on previous reports, which suggested the truncation of the C-terminus of $Ca_V1.2$ channel is required for cAMP-dependent phosphorylation (Bunemann *et al.*, 1999; Fuller *et al.*, 2010; Hulme *et al.*, 2005) and also play a bona fide role in transcriptional regulation (Gomez-Ospina *et al.*, 2006). Based on previous *in vitro* data, we anticipated a similar increased expression of $Ca_V1.2$ in our mouse model. Contrary to our expectations, we found that the homozygous Stop/Stop mice die early after birth. Further analysis of this mouse line by electrophysiology and Western blot indicated that the CMs from Stop/Stop mice displayed a reduced I_{Ba} and $Ca_V1.2$ expression. Severely reduced heart rate and force of contraction were also found, which indicated the low $Ca_V1.2$ channel expression appear to be sufficient for embryonic development but too low to support the physiological up-

regulation of the heart frequency and the force of contraction after birth (Corrigan *et al.*, 2010; Porter *et al.*, 2001). These results explain the cause of the premature death of the Stop/Stop mice. Fu et al. (Fu *et al.*, 2011) achieved similar results with reduced L-type Ca^{2+} current and $Ca_V1.2$ expression in heart of truncated C-terminus Cav1.2 channel after Gly-1796 mouse line. However, mutation at Gly-1796 caused cardiac hypertrophy (Zitieren:Fu et al.). We could not confirm this finding by our morphometric studies in the Stop/Stop mouse line possibly due to the different mutation position. The postpartum death of the Stop/Stop mice was caused by a massive reduction of the $Ca_V1.2$ current and protein expression. As we observed, the current density in Stop/Stop CMs was only 20% of WT/WT CMs. It has been reported that $Ca_V1.2$ proteins are ubiqitinated followed by proteasomal degradation of the translated protein (Altier *et al.*, 2011; Rougier *et al.*, 2011; Waithe *et al.*, 2011). Therefore, we further tried to figure out whether and, if so, to what extent the down-regulated expression of $Ca_V1.2$ can be protected from proteasomal degradation. Further analysis showed that the relative reduction of protein expression and I_{Ba} in the CMs of the Stop/Stop mice were rescued by exposure to bortezomib (10 μM), one kind of proteasome inhibitors which can specifically bind the catalytic site of the 26S proteasome to prevent proteasomal degradation (Bonvini *et al.*, 2007). The low current density in the Stop/Stop CMs was almost 2-fold increased by inhibiton of proteasomal degradation, but still lower than WT/WT CMs. However, we did not anticipate a complete recovery in these experiments because the inhibitors were present for a short time when compared with the expression time of the wild type channel. We did not exceed the time of treatment with the proteasom inhibitors since we observed a significant increase in the number of apoptotic CMs after treatment with the inhibitors longer than 12 h.

In addition, it has been reported that C-terminus of $Ca_V1.2$ serves as the substrate for β-adrenergic regulation of CMs, which can increase the maximal probability of channel opening and Ca^{2+} current amplitude (Bunemann *et al.*, 1999; Catterall, 2000b; Fu *et al.*, 2011; Hulme *et al.*, 2004). Therefore, we extracellularly perfused isoproterenol, a direct activator of β-adrenergic receptor, to investigate β-adrenergic regulation. Isoproterenol can significantly increase I_{Ba} in ventricular CMs from WT and heterozygous mice, but had no effect in Stop/Stop mice. In consideration that robust coupling of β-adrenergic

receptors to G proteins is not fully established until birth (An *et al.*, 1996), the experiments were repeated by FSK, an activator of adenylyl cyclase. Consistent with the isoproterenol data, forskolin doubled I_{Ba} of the WT and heterozygous mice but not that of Stop/Stop mice. Therefore, $Ca_V1.2$ channel truncated after Asp-1904 was not up-regulated by β-adrenergic stimulation in ventricular CMs suggesting that amino acids C-terminal to Aspartate 1904 may be essential for the adrenergic up-regulation of I_{Ca} in the heart.

Truncation of the $Ca_V1.2$ at Asp-1904 in murine will lead to early death of the Stop/Stop mice after birth, because the low concentration of $Ca_V1.2$ channel is not sufficient to support the physiological up-regulation of the heart frequency and contraction after birth. These parameters are even not up-regulated by β-adrenergic stimulation. However, inhibiton of the proteasomal pathway can rescue this low concentration of $Ca_V1.2$ from Stop/Stop mice, which suggests that most of the truncated channel protein is ubiquinated and degraded during transport in the proteasome.

4.2. The role of truncated Cav1.2 at Ser-1905 in transfected HEK293 cells

As already discussed, the homozygous Stop/Stop mice with three stop codons after Asp-1904 in the murine $Ca_V1.2$ gene died after birth caused by a low membrane expression of the $Ca_V1.2$ protein *in vivo*. Next, we examined this concept by the use of the HEK293 cells expression system *in vitro*. HEK293 cells were transfected with the rabbit $Ca_V1.2$ channel isoform HK1 and together with the $Ca_V\beta_{2a}$ and $Ca_V\alpha_2\delta$ subunits. The HK1 sequences were truncated at serine 1905 in rabbbit, corresponding to aspartate 1904 in the murine $Ca_V1.2$ gene, yielding an $HK1^{Stop}$ channel. HEK293 cells transfected with the $HK1^{Stop}$ channel showed low I_{Ba} in electrophysiology analysis and reduced protein expression in immunocytochemical analysis. These results were in contrast with the result of Gao et al. who reported that current density of the C-terminal-truncated mutants at Ser-1905 were significant increased in tsA201 cells (Gao *et al.*, 2000; Gao *et al.*, 2001).

The Western blot analysis supported the notion that there is distinct expression of the truncated isoforms of the $Ca_V1.2$ channel, namely the “cardiac (HK1)” and the “smooth muscle (LK1)” or, alternatively, $Ca_V1.2a$ and $Ca_V1.2b$. Different from HK1, which is

predominantly expressed in CMs, LK1 is mainly expressed in the smooth muscle but not in the CMs. Surprisingly, HEK293 cells transfected with the $LK1^{Stop}$ channel had a robust I_{Ba}. As reported that HK1 and LK1 are alternatively spliced from the same $Ca_V1.2$ channel gene and differ only at four sites, namely, the amino terminus, the IS6 and IVS3 transmembrane segments, and an insert loop connecting domain I and domain II which is only present in the LK1. For further analysis of the "backbone" structure, we introduce LK4 construct which contained the amino-terminal sequence of the LK1 channel on the HK1 backbone for comparision. $LK4^{Stop}$ showed a large I_{Ba} almost as big as $LK1^{Stop}$. These results implied that different behavior between $HK1^{Stop}$ and $LK1^{Stop}$ was possibly caused by the distinct amino terminus. Both LK1 and LK4 contain the amino terminus from the short (exon 1a) smooth muscle isoform, whereas HK1 has the amino terminus from the long (exon 1a) cardiac isoform. These results suggest that the expression of truncated $Ca_V1.2$ channel at Ser-1905 depends on the "backbone" of the channel, *i.e.* whether it contains the amino terminus from the long (exon 1a) cardiac isoform or the shorter (exon1b) smooth muscle isoform.

In consideration that the $Ca_V1.2$ channel allows ubiquitination followed by proteasomal degradation of the protein (Altier *et al.*, 2011; Rougier *et al.*, 2011; Waithe *et al.*, 2011), we speculated that the reduced I_{Ba} of truncated $HK1^{Stop}$ is possibly due to intracellular proteolytic degradation. Therefore, we next examined whether or not inhibition of intracellular proteolysis affected the expression of the $HK1^{Stop}$ channel. To do this, we applied three independent proteasome inhibitors: lactacystin (10 μM), MG132 (10 μM) and bortezomib (10 μM). Electrophysiology revealed a 3-fold increase in I_{Ba} and a significant upregulation in the expression of the $HK1^{Stop}$ protein in HEK293 cells transfected with the $HK1^{Stop}$ channel in the presence of proteasome inhibitors. The I_{Ba} increased by bortezomib can be completely inhibited by the dihydropyridine isradipine. These results suggest that inhibition of the proteasomal pathway rescues partially the expression of the $HK1^{Stop}$ channel.

Actually, the differences in the expression pattern of these two isoforms had already been observed earlier by Welling et al.. She reported that constructs with the long (exon 1a) cardiac amino terminus expressed very poorly in HEK293 cells (Welling *et al.*, 1997). It has been reported that the sequence of carboxyl terminus between 2024 and 2171

contains an inhibitory domain (Gao *et al.*, 2001) which binds to the proximal C-terminus (Singh *et al.*, 2006; Wahl-Schott *et al.*, 2006). Therefore, we speculate that binding of the inhibitory sequence to the proximal C-terminus probably prevents ubiquitination followed by degradation. Truncation of the distal C-terminus maybe change conformation and remove the shield preventing ubiquitination, which was relevant to the cardiac isoform (HK1). Apparently, the short amino terminus of the smooth muscle $Ca_V1.2$ isoform (LK1) induces a conformational shift of the truncated carboxyl terminus that prevents ubiquitination. To some extent, this consideration is supported by several groups that the amino terminus can interact with carboxyl terminus and mutation of the long amino terminus affects PKC modulation (Kobrinsky *et al.*, 2004; Kobrinsky *et al.*, 2005; Shistik *et al.*, 1998).

4.3. The role of truncated $Ca_V1.2$ at Asp-1904 in atrial CMs

Both cardiac ventricle and atrium contribute to effective cardiac function, forming the plateau phase, either ventricular CMs or atrial CMs exhibit robust I_{Ca} that can be enhanced by β-adrenergic stimulation (Anyukhovsky *et al.*, 2002; Brandmayr *et al.*, 2012; Ouadid *et al.*, 1991; Schram *et al.*, 2002). C-terminal truncated forms of the $Ca_V1.2$ channel at Aps-1904 (Stop/Stop mice) results in neonatal death, reduced $Ca_V1.2$ expression and inability to up-regulated the channel by β-adrenergic stimulation in ventricular CMs. Furthermore, truncation of $Ca_V1.2$ sequence at Gly-1796 results also in the inability of the remaining L-type current to be up-regulated by isoproterenol (Fu *et al.*, 2011). However, in contrast to ventricular counterparts, atrial CMs from Stop/Stop mice exhibited robust I_{Ba} that can also be stimulated by the β-adrenergic cascade. This may be partially due to different physiological and anatomical properties as compared with ventricle such as shorter action potentials (Schram *et al.*, 2002), a rudimentary transverse-axial tubular network and different expression levels of key proteins involved in Ca^{2+} signaling (Bootman *et al.*, 2011).

However, further analysis indicated that these currents are mediated by $Ca_V1.3$ channels as evidenced by: i) the characteristic of the current as L-type; ii) the remarkly left shift of the activation curve, since $Ca_V1.3$ channels display a more negative voltage-dependent activation curve as compared with $Ca_V1.2$ channels (Klugbauer *et al.*, 2002; Zhang *et al.*,

2005; Zhang *et al.*, 2002); iii) the reduced inhibition by moderate concentrations of isradipine; and iv) the increased content of the mRNA for $Ca_V1.3$ combined with the unchanged mRNA for $Ca_V1.2a$ and $Ca_V1.2b$. These findings indicate that $Ca_V1.3$ channels partially substitute the loss of the $Ca_V1.2$ channel in atrial but not in ventricular CMs, which is in line with the notion that $Ca_V1.3$ channels may contribute functionally to atrial cardiac CMs (Zhang *et al.*, 2005).

Obviously, the truncation of $Ca_V1.2$ channel at Asp-1904 did not influence the transcription level as our present study showed in pre-natal embros that the expression of $Ca_V1.2$ mRNA was not different between atrium and ventricle from WT and Stop/Stop mice, respectively. This finding further supports the notion that the minor expression of I_{Ba} in ventricular CMs is due to post-translational modifications of the truncated channel. However, expression of $Ca_V1.3$ mRNA was different between atrium and ventricle from WT and Stop/Stop mice. In ventricle, $Ca_V1.3$ mRNA was reduced in Stop/Stop hearts indicating an enhancement of the developmental changes in $Ca_V1.3$ expression towards adulthood. In atrium, $Ca_V1.3$ mRNA was increased in Stop/Stop hearts indicating developmental changes in $Ca_V1.3$ expression towards fetal stages. This result was confirmed by Xu's study that a similar up-regulation of the $Ca_V1.3$ calcium channel was observed in whole embryonic hearts (day E12.5 after conception) from $Ca_V1.2$ deficient mice (Xu *et al.*, 2003). In addition, both Western blot and confocal imaging demonstrated that $Ca_V1.3$ channel protein was expressed in both atrium and ventricle at fetal and, to a less amount, at neonatal stages but was limited to the atrium and absent in the ventricle of the adult heart (Qu *et al.*, 2011).

The C-terminus of the $Ca_V1.2$ channel has been proposed to be a major target site for the β-adrenergic signaling cascade being phosphorylated by the cAMP/PKA pathway (De Jongh *et al.*, 1996). The autoinhibitory complex, consisting of the truncated channel, the cleaved fragment and probably the AKAP, is hypothesized to serve as the substrate for β-adrenergic regulation. The interaction of the cleaved fragment with the rest of the channel reduces ion conduction activity and phosphorylation of serine-1928 then releases this inhibitory interaction (Dai *et al.*, 2009). However, exchange of this amino acid to alanine did not prevent β-adrenergic stimulation of the $Ca_V1.2$ current (Ganesan *et al.*, 2006; Lemke *et al.*, 2008). Recent evidence indicates that the inhibitory interaction may be

instead relieved by PKA-mediated phosphorylation of serine-1700 or threonine-1704 (Fuller *et al.*, 2010). In line with this concept, truncated $Ca_V1.2$ channels in ventricular CMs were unable *in vivo* to respond to β-adrenergic stimulation (Domes *et al.*, 2011; Fu *et al.*, 2011). In the present study, truncated $Ca_V1.2$ channels in atrial CMs shows L-type Ca^{2+} currents. However, these currents seem to be mediate by $Ca_V1.3$ channels and can be stimulated by the β-adrenergic cascade (Qu *et al.*, 2005).

In summary, our results indicate that the $Ca_V1.3$ channel can partially substitute in atrial but in not ventricular CMs the missing $Ca_V1.2$ channel.

5. Summary

The thesis describes the cardiac properties of a mouse line in which the $Ca_V1.2$ gene has been C-terminally truncated after Asp-1904 (Stop/Stop mice). In contrast to studies on the expression of the truncated $Ca_V1.2$ channel in transfected cells, Stop/Stop mice die early after birth, because I_{Ba} and $Ca_V1.2$ protein expression is severely reduced in their cardiac ventricle. Furthermore, $Ca_V1.2$ of the Stop/Stop heart is not up-regulated after birth. The remaining I_{Ca} is too low to support the physiological up-regulation of the heart frequency and the force of contraction. Treatment of ventricular CMs with the proteasome inhibitor bortezomib partially rescued the expression of the truncated channel protein and I_{Ba} in Stop/Stop CMs implying that most of the truncated channel protein was ubiquinated and degraded in the proteasome. In addition, the $Ca_V1.2$ channel truncated after Asp-1904 was not up-regulated by β-adrenergic stimulation in ventricular CMs.

Stop/Stop mice showed a reduced $Ca_V1.2$ expression in the heart but not in smooth muscle samples which finding suggests that the truncated smooth muscle form is protected against proteasomal degradation. To clarify this issue, the cardiac (HK1, $Ca_V1.2a$) and smooth muscle (LK1, $Ca_V1.2b$) isoform was truncated at Ser-1905 ($HK1^{Stop}$ and $LK1^{Stop}$) and expressed together with the β_{2a} and $\alpha_2\delta$ subunit in HEK293 cells. $LK1^{Stop}$ was expressed under this condition, whereas $HK1^{Stop}$ was not. $HK1^{Stop}$ expression was enhanced by the addition of bortezomib. Exchange of the cardiac amino terminus by the smooth muscle amino terminus in $HK1^{Stop}$ led to a solid expression of the chimeric channel.

Since the physiological and anatomical properties differ between ventricle and atrium, we next investigated the expression of $Ca_V1.2$ truncated at Asp-1904 in atrial CMs. Surprisingly and in contrast to ventricular CMs, robust L-type Ca^{2+} currents were observed in atrial CMs from Stop/Stop mice, which were stimulated by the β-adrenergic/cAMP/PKA signaling cascade. Further analysis indicated that these currents are mediated by $Ca_V1.3$ channels as evidenced by i) the characteristic of the current as L-type, ii) the leftward shift of the activation curve, iii) the reduced inhibition by moderate concentrations of isradipine, and iv) the increased content of the mRNA for $Ca_V1.3$ combined with the unchanged mRNA for $Ca_V1.2a$ and $Ca_V1.2b$. These findings indicate

that atrial CMs can partially substitute the failure of $Ca_V1.2$ expression by up-regulating $Ca_V1.3$ expression.

In conclusion, this study shows that truncation of the $Ca_V1.2$ gene at Asp-1904 has tissue-dependent effects: proteasomal degradation of the channel in ventricular CMs, up-regulation of $Ca_V1.3$ in atrial CMs, and no obvious effect on the channel in smooth muscle tissue.

6. References

ADAMS, J. & KAUFFMAN, M. (2004). Development of the proteasome inhibitor Velcade (Bortezomib). *Cancer Invest*, **22,** 304-11.

ALTIER, C., GARCIA-CABALLERO, A., SIMMS, B., YOU, H., CHEN, L., WALCHER, J., TEDFORD, H.W., HERMOSILLA, T. & ZAMPONI, G.W. (2011). The Cavbeta subunit prevents RFP2-mediated ubiquitination and proteasomal degradation of L-type channels. *Nat Neurosci*, **14,** 173-80.

AN, R.H., DAVIES, M.P., DOEVENDANS, P.A., KUBALAK, S.W., BANGALORE, R., CHIEN, K.R. & KASS, R.S. (1996). Developmental changes in beta-adrenergic modulation of L-type Ca2+ channels in embryonic mouse heart. *Circ Res*, **78,** 371-8.

ANYUKHOVSKY, E.P., SOSUNOV, E.A., PLOTNIKOV, A., GAINULLIN, R.Z., JHANG, J.S., MARBOE, C.C. & ROSEN, M.R. (2002). Cellular electrophysiologic properties of old canine atria provide a substrate for arrhythmogenesis. *Cardiovasc Res*, **54,** 462-9.

BEAN, B.P., NOWYCKY, M.C. & TSIEN, R.W. (1984). Beta-adrenergic modulation of calcium channels in frog ventricular heart cells. *Nature*, **307,** 371-5.

BERRIDGE, M.J., LIPP, P. & BOOTMAN, M.D. (2000). The versatility and universality of calcium signalling. *Nat Rev Mol Cell Biol*, **1,** 11-21.

BERS, D.M. (2002). Cardiac excitation-contraction coupling. *Nature*, **415,** 198-205.

BIEL, M., RUTH, P., BOSSE, E., HULLIN, R., STUHMER, W., FLOCKERZI, V. & HOFMANN, F. (1990). Primary structure and functional expression of a high voltage activated calcium channel from rabbit lung. *FEBS Lett*, **269,** 409-12.

BIRNBAUMER, L., CAMPBELL, K.P., CATTERALL, W.A., HARPOLD, M.M., HOFMANN, F., HORNE, W.A., MORI, Y., SCHWARTZ, A., SNUTCH, T.P., TANABE, T. & ET AL. (1994). The naming of voltage-gated calcium channels. *Neuron*, **13,** 505-6.

BLAICH, A., WELLING, A., FISCHER, S., WEGENER, J.W., KOSTNER, K., HOFMANN, F. & MOOSMANG, S. (2010). Facilitation of murine cardiac L-type Ca(v)1.2 channel is modulated by calmodulin kinase II-dependent phosphorylation of S1512 and S1570. *Proc Natl Acad Sci U S A*, **107,** 10285-9.

BOHN, G., MOOSMANG, S., CONRAD, H., LUDWIG, A., HOFMANN, F. & KLUGBAUER, N. (2000). Expression of T- and L-type calcium channel mRNA in murine sinoatrial node. *FEBS Lett*, **481,** 73-6.

BONVINI, P., ZORZI, E., BASSO, G. & ROSOLEN, A. (2007). Bortezomib-mediated 26S proteasome inhibition causes cell-cycle arrest and induces apoptosis in CD-30+ anaplastic large cell lymphoma. *Leukemia*, **21,** 838-42.

BOOTMAN, M.D., SMYRNIAS, I., THUL, R., COOMBES, S. & RODERICK, H.L. (2011). Atrial cardiomyocyte calcium signalling. *Biochim Biophys Acta*, **1813,** 922-34.

BRANDMAYR, J., POOMVANICHA, M., DOMES, K., DING, J., BLAICH, A., WEGENER, J.W., MOOSMANG, S. & HOFMANN, F. (2012). Deletion of the C-terminal phosphorylation sites in the cardiac beta-subunit does not affect the basic

beta-adrenergic response of the heart and the Ca(v)1.2 channel. *J Biol Chem*, **287,** 22584-92.

BUNEMANN, M., GERHARDSTEIN, B.L., GAO, T. & HOSEY, M.M. (1999). Functional regulation of L-type calcium channels via protein kinase A-mediated phosphorylation of the beta(2) subunit. *J Biol Chem*, **274,** 33851-4.

BURNETTE, W.N. (1981). "Western blotting": electrophoretic transfer of proteins from sodium dodecyl sulfate--polyacrylamide gels to unmodified nitrocellulose and radiographic detection with antibody and radioiodinated protein A. *Anal Biochem*, **112,** 195-203.

CATTERALL, W.A. (2000a). From ionic currents to molecular mechanisms: the structure and function of voltage-gated sodium channels. *Neuron*, **26,** 13-25.

CATTERALL, W.A. (2000b). Structure and regulation of voltage-gated Ca2+ channels. *Annu Rev Cell Dev Biol*, **16,** 521-55.

CATTERALL, W.A. & FEW, A.P. (2008). Calcium channel regulation and presynaptic plasticity. *Neuron*, **59,** 882-901.

CHENG, X., LIU, J., ASUNCION-CHIN, M., BLASKOVA, E., BANNISTER, J.P., DOPICO, A.M. & JAGGAR, J.H. (2007). A novel Ca(V)1.2 N terminus expressed in smooth muscle cells of resistance size arteries modifies channel regulation by auxiliary subunits. *J Biol Chem*, **282,** 29211-21.

CLAPHAM, D.E. (1995). Calcium signaling. *Cell*, **80,** 259-68.

CORRIGAN, N., BRAZIL, D.P. & AULIFFE, F.M. (2010). High-frequency ultrasound assessment of the murine heart from embryo through to juvenile. *Reprod Sci*, **17,** 147-57.

DAI, S., HALL, D.D. & HELL, J.W. (2009). Supramolecular assemblies and localized regulation of voltage-gated ion channels. *Physiol Rev*, **89,** 411-52.

DAVARE, M.A., AVDONIN, V., HALL, D.D., PEDEN, E.M., BURETTE, A., WEINBERG, R.J., HORNE, M.C., HOSHI, T. & HELL, J.W. (2001). A beta2 adrenergic receptor signaling complex assembled with the Ca2+ channel Cav1.2. *Science*, **293,** 98-101.

DE JONGH, K.S., MURPHY, B.J., COLVIN, A.A., HELL, J.W., TAKAHASHI, M. & CATTERALL, W.A. (1996). Specific phosphorylation of a site in the full-length form of the alpha 1 subunit of the cardiac L-type calcium channel by adenosine 3',5'-cyclic monophosphate-dependent protein kinase. *Biochemistry*, **35,** 10392-402.

DE JONGH, K.S., WARNER, C., COLVIN, A.A. & CATTERALL, W.A. (1991). Characterization of the two size forms of the alpha 1 subunit of skeletal muscle L-type calcium channels. *Proc Natl Acad Sci U S A*, **88,** 10778-82.

DE WAARD, M., GURNETT, C.A. & CAMPBELL, K.P. (1996). Structural and functional diversity of voltage-activated calcium channels. *Ion Channels*, **4,** 41-87.

DEMARIA, C.D., SOONG, T.W., ALSEIKHAN, B.A., ALVANIA, R.S. & YUE, D.T. (2001). Calmodulin bifurcates the local Ca2+ signal that modulates P/Q-type Ca2+ channels. *Nature*, **411,** 484-9.

DOLMETSCH, R.E., PAJVANI, U., FIFE, K., SPOTTS, J.M. & GREENBERG, M.E. (2001). Signaling to the nucleus by an L-type calcium channel-calmodulin complex through the MAP kinase pathway. *Science*, **294,** 333-9.

DOLPHIN, A.C. (2012a). The alpha(2)delta subunits of voltage-gated calcium channels. *Biochim Biophys Acta*, **2736,** 00410-5.

DOLPHIN, A.C. (2012b). Calcium channel auxiliary alpha2delta and beta subunits: trafficking and one step beyond. *Nat Rev Neurosci*, **13,** 542-55.

DOMES, K., DING, J., LEMKE, T., BLAICH, A., WEGENER, J.W., BRANDMAYR, J., MOOSMANG, S. & HOFMANN, F. (2011). Truncation of murine CaV1.2 at Asp-1904 results in heart failure after birth. *J Biol Chem*, **286,** 33863-71.

DZHURA, I., WU, Y., COLBRAN, R.J., BALSER, J.R. & ANDERSON, M.E. (2000). Calmodulin kinase determines calcium-dependent facilitation of L-type calcium channels. *Nat Cell Biol*, **2,** 173-7.

ERTEL, E.A., CAMPBELL, K.P., HARPOLD, M.M., HOFMANN, F., MORI, Y., PEREZ-REYES, E., SCHWARTZ, A., SNUTCH, T.P., TANABE, T., BIRNBAUMER, L., TSIEN, R.W. & CATTERALL, W.A. (2000). Nomenclature of voltage-gated calcium channels. *Neuron*, **25,** 533-5.

ESCAYG, A., MACDONALD, B.T., MEISLER, M.H., BAULAC, S., HUBERFELD, G., AN-GOURFINKEL, I., BRICE, A., LEGUERN, E., MOULARD, B., CHAIGNE, D., BURESI, C. & MALAFOSSE, A. (2000). Mutations of SCN1A, encoding a neuronal sodium channel, in two families with GEFS+2. *Nat Genet*, **24,** 343-5.

FU, Y., WESTENBROEK, R.E., YU, F.H., CLARK, J.P., 3RD, MARSHALL, M.R., SCHEUER, T. & CATTERALL, W.A. (2011). Deletion of the distal C terminus of CaV1.2 channels leads to loss of beta-adrenergic regulation and heart failure in vivo. *J Biol Chem*, **286,** 12617-26.

FULLER, M.D., EMRICK, M.A., SADILEK, M., SCHEUER, T. & CATTERALL, W.A. (2010). Molecular mechanism of calcium channel regulation in the fight-or-flight response. *Sci Signal*, **3,** ra70.

GABORIT, N., LE BOUTER, S., SZUTS, V., VARRO, A., ESCANDE, D., NATTEL, S. & DEMOLOMBE, S. (2007). Regional and tissue specific transcript signatures of ion channel genes in the non-diseased human heart. *J Physiol*, **582,** 675-93.

GANESAN, A.N., MAACK, C., JOHNS, D.C., SIDOR, A. & O'ROURKE, B. (2006). Beta-adrenergic stimulation of L-type Ca2+ channels in cardiac myocytes requires the distal carboxyl terminus of alpha1C but not serine 1928. *Circ Res*, **98,** e11-8.

GAO, T., BUNEMANN, M., GERHARDSTEIN, B.L., MA, H. & HOSEY, M.M. (2000). Role of the C terminus of the alpha 1C (CaV1.2) subunit in membrane targeting of cardiac L-type calcium channels. *J Biol Chem*, **275,** 25436-44.

GAO, T., CUADRA, A.E., MA, H., BUNEMANN, M., GERHARDSTEIN, B.L., CHENG, T., EICK, R.T. & HOSEY, M.M. (2001). C-terminal fragments of the alpha 1C (CaV1.2) subunit associate with and regulate L-type calcium channels containing C-terminal-truncated alpha 1C subunits. *J Biol Chem*, **276,** 21089-97.

GERHARDSTEIN, B.L., PURI, T.S., CHIEN, A.J. & HOSEY, M.M. (1999). Identification of the sites phosphorylated by cyclic AMP-dependent protein kinase on the beta 2 subunit of L-type voltage-dependent calcium channels. *Biochemistry*, **38,** 10361-70.

GHOSH, A. & GREENBERG, M.E. (1995). Calcium signaling in neurons: molecular mechanisms and cellular consequences. *Science*, **268,** 239-47.

GOMEZ-OSPINA, N., TSURUTA, F., BARRETO-CHANG, O., HU, L. & DOLMETSCH, R. (2006). The C terminus of the L-type voltage-gated calcium channel Ca(V)1.2 encodes a transcription factor. *Cell*, **127,** 591-606.

GOMEZ, A.M., VALDIVIA, H.H., CHENG, H., LEDERER, M.R., SANTANA, L.F., CANNELL, M.B., MCCUNE, S.A., ALTSCHULD, R.A. & LEDERER, W.J. (1997). Defective excitation-contraction coupling in experimental cardiac hypertrophy and heart failure. *Science*, **276,** 800-6.

GUY, H.R. & CONTI, F. (1990). Pursuing the structure and function of voltage-gated channels. *Trends Neurosci*, **13,** 201-6.

HAGIWARA, S., OZAWA, S. & SAND, O. (1975). Voltage clamp analysis of two inward current mechanisms in the egg cell membrane of a starfish. *J Gen Physiol*, **65,** 617-44.

HAMILL, O.P., MARTY, A., NEHER, E., SAKMANN, B. & SIGWORTH, F.J. (1981). Improved patch-clamp techniques for high-resolution current recording from cells and cell-free membrane patches. *Pflugers Arch*, **391,** 85-100.

HAMILTON, S.L., YATANI, A., BRUSH, K., SCHWARTZ, A. & BROWN, A.M. (1987). A comparison between the binding and electrophysiological effects of dihydropyridines on cardiac membranes. *Mol Pharmacol*, **31,** 221-31.

HE, J., CONKLIN, M.W., FOELL, J.D., WOLFF, M.R., HAWORTH, R.A., CORONADO, R. & KAMP, T.J. (2001). Reduction in density of transverse tubules and L-type Ca(2+) channels in canine tachycardia-induced heart failure. *Cardiovasc Res*, **49,** 298-307.

HELL, J.W., WESTENBROEK, R.E., WARNER, C., AHLIJANIAN, M.K., PRYSTAY, W., GILBERT, M.M., SNUTCH, T.P. & CATTERALL, W.A. (1993). Identification and differential subcellular localization of the neuronal class C and class D L-type calcium channel alpha 1 subunits. *J Cell Biol*, **123,** 949-62.

HOPPA, M.B., LANA, B., MARGAS, W., DOLPHIN, A.C. & RYAN, T.A. (2012). alpha2delta expression sets presynaptic calcium channel abundance and release probability. *Nature*, **486,** 122-5.

HU, H. & MARBAN, E. (1998). Isoform-specific inhibition of L-type calcium channels by dihydropyridines is independent of isoform-specific gating properties. *Mol Pharmacol*, **53,** 902-7.

HULLIN, R., SINGER-LAHAT, D., FREICHEL, M., BIEL, M., DASCAL, N., HOFMANN, F. & FLOCKERZI, V. (1992). Calcium channel beta subunit heterogeneity: functional expression of cloned cDNA from heart, aorta and brain. *EMBO J*, **11,** 885-90.

HULME, J.T., KONOKI, K., LIN, T.W., GRITSENKO, M.A., CAMP, D.G., 2ND, BIGELOW, D.J. & CATTERALL, W.A. (2005). Sites of proteolytic processing and noncovalent association of the distal C-terminal domain of CaV1.1 channels in skeletal muscle. *Proc Natl Acad Sci U S A*, **102,** 5274-9.

HULME, J.T., LIN, T.W., WESTENBROEK, R.E., SCHEUER, T. & CATTERALL, W.A. (2003). Beta-adrenergic regulation requires direct anchoring of PKA to cardiac CaV1.2 channels via a leucine zipper interaction with A kinase-anchoring protein 15. *Proc Natl Acad Sci U S A*, **100,** 13093-8.

HULME, J.T., SCHEUER, T. & CATTERALL, W.A. (2004). Regulation of cardiac ion channels by signaling complexes: role of modified leucine zipper motifs. *J Mol Cell Cardiol*, **37,** 625-31.

HULME, J.T., WESTENBROEK, R.E., SCHEUER, T. & CATTERALL, W.A. (2006a). Phosphorylation of serine 1928 in the distal C-terminal domain of cardiac CaV1.2 channels during beta1-adrenergic regulation. *Proc Natl Acad Sci U S A*, **103,** 16574-9.

HULME, J.T., YAROV-YAROVOY, V., LIN, T.W., SCHEUER, T. & CATTERALL, W.A. (2006b). Autoinhibitory control of the CaV1.2 channel by its proteolytically processed distal C-terminal domain. *J Physiol*, **576,** 87-102.

JONES, B.W., BRUNET, S., GILBERT, M.L., NICHOLS, C.B., SU, T., WESTENBROEK, R.E., SCOTT, J.D., CATTERALL, W.A. & MCKNIGHT, G.S. (2012). Cardiomyocytes from AKAP7 knockout mice respond normally to adrenergic stimulation. *Proc Natl Acad Sci U S A*, **109,** 17099-104.

JOSEPHSON, I.R. & VARADI, G. (1996). The beta subunit increases Ca2+ currents and gating charge movements of human cardiac L-type Ca2+ channels. *Biophys J*, **70,** 1285-93.

KAMP, T.J., PEREZ-GARCIA, M.T. & MARBAN, E. (1996). Enhancement of ionic current and charge movement by coexpression of calcium channel beta 1A subunit with alpha 1C subunit in a human embryonic kidney cell line. *J Physiol*, **492 (Pt 1),** 89-96.

KEPPLINGER, K.J., KAHR, H., FORSTNER, G., SONNLEITNER, M., SCHINDLER, H., SCHMIDT, T., GROSCHNER, K., SOLDATOV, N.M. & ROMANIN, C. (2000). A sequence in the carboxy-terminus of the alpha(1C) subunit important for targeting, conductance and open probability of L-type Ca(2+) channels. *FEBS Lett*, **477,** 161-9.

KLUGBAUER, N., DAI, S., SPECHT, V., LACINOVA, L., MARAIS, E., BOHN, G. & HOFMANN, F. (2000). A family of gamma-like calcium channel subunits. *FEBS Lett*, **470,** 189-97.

KLUGBAUER, N., WELLING, A., SPECHT, V., SEISENBERGER, C. & HOFMANN, F. (2002). L-type Ca2+ channels of the embryonic mouse heart. *Eur J Pharmacol*, **447,** 279-84.

KOBRINSKY, E., KEPPLINGER, K.J., YU, A., HARRY, J.B., KAHR, H., ROMANIN, C., ABERNETHY, D.R. & SOLDATOV, N.M. (2004). Voltage-gated rearrangements associated with differential beta-subunit modulation of the L-type Ca(2+) channel inactivation. *Biophys J*, **87,** 844-57.

KOBRINSKY, E., TIWARI, S., MALTSEV, V.A., HARRY, J.B., LAKATTA, E., ABERNETHY, D.R. & SOLDATOV, N.M. (2005). Differential role of the alpha1C subunit tails in regulation of the Cav1.2 channel by membrane potential, beta subunits, and Ca2+ ions. *J Biol Chem*, **280,** 12474-85.

KOSCHAK, A., REIMER, D., HUBER, I., GRABNER, M., GLOSSMANN, H., ENGEL, J. & STRIESSNIG, J. (2001). alpha 1D (Cav1.3) subunits can form l-type Ca2+ channels activating at negative voltages. *J Biol Chem*, **276,** 22100-6.

LACINOVA, L. (2005). Voltage-dependent calcium channels. *Gen Physiol Biophys*, **24 Suppl 1,** 1-78.

LEE, T.S., KARL, R., MOOSMANG, S., LENHARDT, P., KLUGBAUER, N., HOFMANN, F., KLEPPISCH, T. & WELLING, A. (2006). Calmodulin kinase II is involved in voltage-dependent facilitation of the L-type Cav1.2 calcium channel: Identification of the phosphorylation sites. *J Biol Chem*, **281,** 25560-7.

LEMKE, T., WELLING, A., CHRISTEL, C.J., BLAICH, A., BERNHARD, D., LENHARDT, P., HOFMANN, F. & MOOSMANG, S. (2008). Unchanged beta-adrenergic stimulation of cardiac L-type calcium channels in Ca v 1.2 phosphorylation site S1928A mutant mice. *J Biol Chem*, **283,** 34738-44.

LETTS, V.A., FELIX, R., BIDDLECOME, G.H., ARIKKATH, J., MAHAFFEY, C.L., VALENZUELA, A., BARTLETT, F.S., 2ND, MORI, Y., CAMPBELL, K.P. & FRANKEL, W.N. (1998). The mouse stargazer gene encodes a neuronal Ca2+-channel gamma subunit. *Nat Genet*, **19,** 340-7.

LINK, S., MEISSNER, M., HELD, B., BECK, A., WEISSGERBER, P., FREICHEL, M. & FLOCKERZI, V. (2009). Diversity and developmental expression of L-type calcium channel beta2 proteins and their influence on calcium current in murine heart. *J Biol Chem*, **284,** 30129-37.

LIPSCOMBE, D. (2002). L-type calcium channels: highs and new lows. *Circ Res*, **90,** 933-5.

LLINAS, R. & YAROM, Y. (1981). Electrophysiology of mammalian inferior olivary neurones in vitro. Different types of voltage-dependent ionic conductances. *J Physiol*, **315,** 549-67.

MARCANTONI, A., BALDELLI, P., HERNANDEZ-GUIJO, J.M., COMUNANZA, V., CARABELLI, V. & CARBONE, E. (2007). L-type calcium channels in adrenal chromaffin cells: role in pace-making and secretion. *Cell Calcium*, **42,** 397-408.

MCRORY, J.E., HAMID, J., DOERING, C.J., GARCIA, E., PARKER, R., HAMMING, K., CHEN, L., HILDEBRAND, M., BEEDLE, A.M., FELDCAMP, L., ZAMPONI, G.W. & SNUTCH, T.P. (2004). The CACNA1F gene encodes an L-type calcium channel with unique biophysical properties and tissue distribution. *J Neurosci*, **24,** 1707-18.

MIKAMI, A., IMOTO, K., TANABE, T., NIIDOME, T., MORI, Y., TAKESHIMA, H., NARUMIYA, S. & NUMA, S. (1989). Primary structure and functional expression of the cardiac dihydropyridine-sensitive calcium channel. *Nature*, **340,** 230-3.

MOOSMANG, S., SCHULLA, V., WELLING, A., FEIL, R., FEIL, S., WEGENER, J.W., HOFMANN, F. & KLUGBAUER, N. (2003). Dominant role of smooth muscle L-type calcium channel Cav1.2 for blood pressure regulation. *EMBO J*, **22,** 6027-34.

NAKADA, T., FLUCHER, B.E., KASHIHARA, T., SHENG, X., SHIBAZAKI, T., HORIUCHI-HIROSE, M., GOMI, S., HIROSE, M. & YAMADA, M. (2012). Proximal C-

terminus of alpha1C subunits is necessary for junctional membrane-targeting of cardiac L-type calcium channels. *Biochem J*.

NEELY, A., WEI, X., OLCESE, R., BIRNBAUMER, L. & STEFANI, E. (1993). Potentiation by the beta subunit of the ratio of the ionic current to the charge movement in the cardiac calcium channel. *Science*, **262,** 575-8.

NEHER, E. & SAKMANN, B. (1992). The patch clamp technique. *Sci Am*, **266,** 44-51.

OSTERRIEDER, W., BRUM, G., HESCHELER, J., TRAUTWEIN, W., FLOCKERZI, V. & HOFMANN, F. (1982). Injection of subunits of cyclic AMP-dependent protein kinase into cardiac myocytes modulates Ca2+ current. *Nature*, **298,** 576-8.

OUADID, H., SEGUIN, J., RICHARD, S., CHAPTAL, P.A. & NARGEOT, J. (1991). Properties and Modulation of Ca channels in adult human atrial cells. *J Mol Cell Cardiol*, **23,** 41-54.

OZAWA, M. (1995). Structure of the gene encoding mouse reticulocalbin, a novel endoplasmic reticulum-resident Ca(2+)-binding protein with multiple EF-hand motifs. *J Biochem*, **118,** 154-60.

PETERSON, B.Z., DEMARIA, C.D., ADELMAN, J.P. & YUE, D.T. (1999). Calmodulin is the Ca2+ sensor for Ca2+ -dependent inactivation of L-type calcium channels. *Neuron*, **22,** 549-58.

POGWIZD, S.M., SCHLOTTHAUER, K., LI, L., YUAN, W. & BERS, D.M. (2001). Arrhythmogenesis and contractile dysfunction in heart failure: Roles of sodium-calcium exchange, inward rectifier potassium current, and residual beta-adrenergic responsiveness. *Circ Res*, **88,** 1159-67.

PORTER, G.A., JR. & RIVKEES, S.A. (2001). Ontogeny of humoral heart rate regulation in the embryonic mouse. *Am J Physiol Regul Integr Comp Physiol*, **281,** R401-7.

QU, Y., BAROUDI, G., YUE, Y., EL-SHERIF, N. & BOUTJDIR, M. (2005). Localization and modulation of {alpha}1D (Cav1.3) L-type Ca channel by protein kinase A. *American journal of physiology. Heart and circulatory physiology*, **288,** H2123-30.

QU, Y., KARNABI, E., RAMADAN, O., YUE, Y., CHAHINE, M. & BOUTJDIR, M. (2011). Perinatal and postnatal expression of Cav1.3 alpha1D Ca(2)(+) channel in the rat heart. *Pediatr Res*, **69,** 479-84.

REUTER, H. (1983). Calcium channel modulation by neurotransmitters, enzymes and drugs. *Nature*, **301,** 569-74.

ROUGIER, J.S., ALBESA, M., ABRIEL, H. & VIARD, P. (2011). Neuronal precursor cell-expressed developmentally down-regulated 4-1 (NEDD4-1) controls the sorting of newly synthesized Ca(V)1.2 calcium channels. *J Biol Chem*, **286,** 8829-38.

SCHRAM, G., POURRIER, M., MELNYK, P. & NATTEL, S. (2002). Differential distribution of cardiac ion channel expression as a basis for regional specialization in electrical function. *Circ Res*, **90,** 939-50.

SCHRODER, F., HANDROCK, R., BEUCKELMANN, D.J., HIRT, S., HULLIN, R., PRIEBE, L., SCHWINGER, R.H., WEIL, J. & HERZIG, S. (1998). Increased availability and open probability of single L-type calcium channels from failing compared with nonfailing human ventricle. *Circulation*, **98,** 969-76.

SCHULLA, V., RENSTROM, E., FEIL, R., FEIL, S., FRANKLIN, I., GJINOVCI, A., JING, X.J., LAUX, D., LUNDQUIST, I., MAGNUSON, M.A., OBERMULLER, S., OLOFSSON, C.S., SALEHI, A., WENDT, A., KLUGBAUER, N., WOLLHEIM, C.B., RORSMAN, P. & HOFMANN, F. (2003). Impaired insulin secretion and glucose tolerance in beta cell-selective Ca(v)1.2 Ca2+ channel null mice. *EMBO J*, **22,** 3844-54.

SEINO, S., CHEN, L., SEINO, M., BLONDEL, O., TAKEDA, J., JOHNSON, J.H. & BELL, G.I. (1992). Cloning of the alpha 1 subunit of a voltage-dependent calcium channel expressed in pancreatic beta cells. *Proc Natl Acad Sci U S A*, **89,** 584-8.

SEISENBERGER, C., SPECHT, V., WELLING, A., PLATZER, J., PFEIFER, A., KUHBANDNER, S., STRIESSNIG, J., KLUGBAUER, N., FEIL, R. & HOFMANN, F. (2000). Functional embryonic cardiomyocytes after disruption of the L-type alpha1C (Cav1.2) calcium channel gene in the mouse. *J Biol Chem*, **275,** 39193-9.

SHISTIK, E., IVANINA, T., BLUMENSTEIN, Y. & DASCAL, N. (1998). Crucial role of N terminus in function of cardiac L-type Ca2+ channel and its modulation by protein kinase C. *J Biol Chem*, **273,** 17901-9.

SINGER, D., BIEL, M., LOTAN, I., FLOCKERZI, V., HOFMANN, F. & DASCAL, N. (1991). The roles of the subunits in the function of the calcium channel. *Science*, **253,** 1553-7.

SINGH, A., HAMEDINGER, D., HODA, J.C., GEBHART, M., KOSCHAK, A., ROMANIN, C. & STRIESSNIG, J. (2006). C-terminal modulator controls Ca2+-dependent gating of Ca(v)1.4 L-type Ca2+ channels. *Nat Neurosci*, **9,** 1108-16.

SNUTCH, T.P., LEONARD, J.P., GILBERT, M.M., LESTER, H.A. & DAVIDSON, N. (1990). Rat brain expresses a heterogeneous family of calcium channels. *Proc Natl Acad Sci U S A*, **87,** 3391-5.

STRIESSNIG, J. (1999). Pharmacology, structure and function of cardiac L-type Ca(2+) channels. *Cell Physiol Biochem*, **9,** 242-69.

STROM, T.M., NYAKATURA, G., APFELSTEDT-SYLLA, E., HELLEBRAND, H., LORENZ, B., WEBER, B.H., WUTZ, K., GUTWILLINGER, N., RUTHER, K., DRESCHER, B., SAUER, C., ZRENNER, E., MEITINGER, T., ROSENTHAL, A. & MEINDL, A. (1998). An L-type calcium-channel gene mutated in incomplete X-linked congenital stationary night blindness. *Nat Genet*, **19,** 260-3.

TANABE, T., TAKESHIMA, H., MIKAMI, A., FLOCKERZI, V., TAKAHASHI, H., KANGAWA, K., KOJIMA, M., MATSUO, H., HIROSE, T. & NUMA, S. (1987). Primary structure of the receptor for calcium channel blockers from skeletal muscle. *Nature*, **328,** 313-8.

TOWBIN, H., STAEHELIN, T. & GORDON, J. (1979). Electrophoretic transfer of proteins from polyacrylamide gels to nitrocellulose sheets: procedure and some applications. *Proc Natl Acad Sci U S A*, **76,** 4350-4.

TSIEN, R.W., LIPSCOMBE, D., MADISON, D.V., BLEY, K.R. & FOX, A.P. (1988). Multiple types of neuronal calcium channels and their selective modulation. *Trends Neurosci*, **11,** 431-8.

VAN PETEGEM, F., CHATELAIN, F.C. & MINOR, D.L., JR. (2005). Insights into voltage-gated calcium channel regulation from the structure of the CaV1.2 IQ domain-Ca2+/calmodulin complex. *Nat Struct Mol Biol*, **12,** 1108-15.

WAHL-SCHOTT, C., BAUMANN, L., CUNY, H., ECKERT, C., GRIESSMEIER, K. & BIEL, M. (2006). Switching off calcium-dependent inactivation in L-type calcium channels by an autoinhibitory domain. *Proc Natl Acad Sci U S A*, **103,** 15657-62.

WAITHE, D., FERRON, L., PAGE, K.M., CHAGGAR, K. & DOLPHIN, A.C. (2011). Beta-subunits promote the expression of Ca(V)2.2 channels by reducing their proteasomal degradation. *J Biol Chem*, **286,** 9598-611.

WEGENER, J.W., SCHULLA, V., KOLLER, A., KLUGBAUER, N., FEIL, R. & HOFMANN, F. (2006). Control of intestinal motility by the Ca(v)1.2 L-type calcium channel in mice. *FASEB J*, **20,** 1260-2.

WEGENER, J.W., SCHULLA, V., LEE, T.S., KOLLER, A., FEIL, S., FEIL, R., KLEPPISCH, T., KLUGBAUER, N., MOOSMANG, S., WELLING, A. & HOFMANN, F. (2004). An essential role of Cav1.2 L-type calcium channel for urinary bladder function. *FASEB J*, **18,** 1159-61.

WEI, X., NEELY, A., LACERDA, A.E., OLCESE, R., STEFANI, E., PEREZ-REYES, E. & BIRNBAUMER, L. (1994). Modification of Ca2+ channel activity by deletions at the carboxyl terminus of the cardiac alpha 1 subunit. *J Biol Chem*, **269,** 1635-40.

WELLING, A., LUDWIG, A., ZIMMER, S., KLUGBAUER, N., FLOCKERZI, V. & HOFMANN, F. (1997). Alternatively spliced IS6 segments of the alpha 1C gene determine the tissue-specific dihydropyridine sensitivity of cardiac and vascular smooth muscle L-type Ca2+ channels. *Circ Res*, **81,** 526-32.

XU, M., WELLING, A., PAPARISTO, S., HOFMANN, F. & KLUGBAUER, N. (2003). Enhanced expression of L-type Cav1.3 calcium channels in murine embryonic hearts from Cav1.2-deficient mice. *J Biol Chem*, **278,** 40837-41.

ZHANG, Z., HE, Y., TUTEJA, D., XU, D., TIMOFEYEV, V., ZHANG, Q., GLATTER, K.A., XU, Y., SHIN, H.S., LOW, R. & CHIAMVIMONVAT, N. (2005). Functional roles of Cav1.3(alpha1D) calcium channels in atria: insights gained from gene-targeted null mutant mice. *Circulation*, **112,** 1936-44.

ZHANG, Z., XU, Y., SONG, H., RODRIGUEZ, J., TUTEJA, D., NAMKUNG, Y., SHIN, H.S. & CHIAMVIMONVAT, N. (2002). Functional Roles of Ca(v)1.3 (alpha(1D)) calcium channel in sinoatrial nodes: insight gained using gene-targeted null mutant mice. *Circ Res*, **90,** 981-7.

ZHOU, H.Y., TAN, Y.Y., WANG, Z.Q., WANG, G., LU, G.Q. & CHEN, S.D. (2010). Proteasome inhibitor lactacystin induces cholinergic degeneration. *Can J Neurol Sci*, **37,** 229-34.

ZUHLKE, R.D., PITT, G.S., DEISSEROTH, K., TSIEN, R.W. & REUTER, H. (1999). Calmodulin supports both inactivation and facilitation of L-type calcium channels. *Nature*, **399,** 159-62.

ZUHLKE, R.D., PITT, G.S., TSIEN, R.W. & REUTER, H. (2000). Ca2+-sensitive inactivation and facilitation of L-type Ca2+ channels both depend on

specific amino acid residues in a consensus calmodulin-binding motif in the(alpha)1C subunit. *J Biol Chem*, **275,** 21121-9.

Results of this thesis have been partially published or submitted

1. Ding J, Domes K, Hofmann F, Wegener JW (2012). Truncation of murine $Ca_V1.2$ at Asp 1904 increases $Ca_V1.3$ expression in embryonic atrial cardiomyocytes. *Pflügers Archiv - European Journal of Physiology* (*accepted*)

2. Brandmayr J, Poomvanicha M, Domes K, Ding J, Blaich A, Wegener JW, Moosmang S, Hofmann F (2012). Deletion of the C-terminal phosphorylation sites in the cardiac beta-subunit does not affect the basic beta-adrenergic response of the heart and the Ca(v)1.2 channel. *J Biol Chem* **287**(27)**:** 22584-22592

3. Domes K, Ding J, Lemke T, Blaich A, Wegener JW, Brandmayr J, Moosmang S, Hofmann F (2011). Truncation of murine $Ca_V1.2$ at Asp-1904 results in heart failure after birth. *J Biol Chem* **286**(39)**:** 33863-33871

Curriculum Vitae

Personal Data

Name	Jie Ding
Date of birth	17 March 1983
Nationality	China

Education

10/2009-	Ph.D. (Pharmacology) Institute of Pharmacology and Toxicology, Technical University of Munich, Germany
09/2007-07/2009	M.S. (Pharmacology) Tongji Medical college Huazhong University of Science and Technology, China
09/2002-07/2007	B.S. (Pharmacy) Tongji Medical college Huazhong University of Science and Technology, China

Honors and awards

2003	the Second-rate Scholarship, HUST
2006	Award for Excellent Student Leader, HUST
2007	Award for Excellent Graduate Student, HUST
2007	the nutritionist be eligible for certification

Publications

1. Qin Li, Xian-Ju Huang, Wei He, Jie Ding, Jun-Ting Jia, Gang Fu, Hong-Xing Wang, Lian-Jun Guo (2009). Neuroprotective potential of fasudil mesylate in brain ischemia-reperfusion injury of rats. *Cell Mol Neurobiol* 29:169-180 DOI 10.1007/s10571-008-9308-8

2. Domes K, Ding J, Lemke T, Blaich A, Wegener JW, Brandmayr J, Moosmang S, Hofmann F (2011). Truncation of murine CaV1.2 at Asp-1904 results in heart failure after birth. *J Biol Chem* **286**(39)**:** 33863-33871

3. Ding J, Fu G, Zhao Y, Guo LJ. (2011). EGCG ameliorates the suppression of long-term potentiation induced by ischemia at the Schaffer collateral-CA1 synapse in the rat. *Cell Mol Neurobiol* DOI 10.1007/s10571-011-9758-2

4. Brandmayr J, Poomvanicha M, Domes K, Ding J, Blaich A, Wegener JW, Moosmang S, Hofmann F (2012). Deletion of the C-terminal phosphorylation sites in the cardiac beta-subunit does not affect the basic beta-adrenergic response of the heart and the Ca(v)1.2 channel. *J Biol Chem* **287**(27)**:** 22584-22592

5. Zhao B, Chen Y, Sun X, Zhou M, Ding J, Zhan JJ, Guo LJ. (2012) Phenolic alkaloids from Menispermum dauricum rhizome protect against brain ischemia injury via regulation of GLT-1, EAAC1 and ROS generation. *Molecules* Mar 6; 17(3):2725-37

6. Ding J, Domes K, Hofmann F, Wegener JW. (2012). Truncation of murine $Ca_V1.2$ at Asp 1904 increases $Ca_V1.3$ expression in embryonic atrial cardiomyocytes. *Pflügers Archiv - European Journal of Physiology* (*under review*)

Thesis

Functional Analysis of Truncated Murine Cav1.2 at Asp-1904 in hearts

Acknowledgements

At this point I would like to thank all those persons who have contributed to making this work:

I am very grateful to Prof. Dr. Franz Hofmann for giving me the opportunity to study and pursue the doctoral thesis in the Institute of Pharmacology and Toxicology, Technical University of Munich. The valuable supervision, guidance and support from Prof. Dr. Franz Hofmann for this project are greatly appreciated.

Special thanks are given to my thesis committee, especially to Prof. Dr. Michael Schemann for being my doctor father.

A lot of thanks go to PD Dr. Jörg Wegener for his patience, technical suppot, suggestion and introduction to various experimental techniques during my study.

I would like to sincerely thank Dr. Toni Lemke and Dr. Katrin Domes who performed the mutation and Westen blot experiments in this thesis.

A huge thanks to Montatip Poomvanicha, Florian Loga and Enrico Patrucco for their friendly atmosphere in the office, the fun time we spent together inside or outside the laboratory is precious. I also would like to thank Anne, Bea, Tea, Memo, Stefanie and Elisabeth for the friendly atmosphere in the laboratory and for giving me a hand in the experiment.

I greatly acknowledge Faculty of Neuropharmacology, Tongji Medical College, Huazhong University of Science & Technology (HUST) where my former professors and friends continue to show their care and support for me during my study in Germany. Special thanks are given to Prof. Dr. Xiangang Zong and his family for the help and care during my study in Munich.

Finally, my heartful thanks to my parents for their endless trust and support they have given me during my study. I thank everyone in the Institute of Pharmacology and Toxicology, Technical University of Munich for their help and friendliness.